CONTRACTOR REPORT

SAND83—7466
Unlimited Release
UC—70

Preliminary Two-Dimensional Regional Hydrologic Model of the Nevada Test Site and Vicinity

W. A. Rice
Pacific Northwest Laboratory
Richland, WA 99352

Prepared by Sandia National Laboratories Albuquerque, New Mexico 87185 and Livermore, California 94550 for the United States Department of Energy under Contract DE-AC04-76DP00789

Printed August 1984

HYDROLOGY DOCUMENT NUMBER 549

Issued by Sandia National Laboratories, operated for the United States Department of Energy by Sandia Corporation.

NOTICE: This report was prepared as an account of work sponsored by an agency of the United States Government. Neither the United States Government nor any agency thereof, nor any of their employees, nor any of their contractors, subcontractors, or their employees, makes any warranty, express or implied, or assumes any legal liability or responsibility for the accuracy, completeness, or usefulness of any information, apparatus, product, or process disclosed, or represents that its use would not infringe privately owned rights. Reference herein to any specific commercial product, process, or service by trade name, trademark, manufacturer, or otherwise, does not necessarily constitute or imply its endorsement, recommendation, or favoring by the United States Government, any agency thereof or any of their contractors or subcontractors. The views and opinions expressed herein do not necessarily state or reflect those of the United States Government, any agency thereof or any of their contractors or subcontractors.

Printed in the United States of America
Available from
National Technical Information Service
U.S. Department of Commerce
5285 Port Royal Road
Springfield, VA 22161

NTIS price codes
Printed copy: A05
Microfiche copy: A01

SAND83–7466
Unlimited Release
Printed August 1984

Distribution
Category UC–70

Preliminary Two-Dimensional Regional Hydrologic Model of the Nevada Test Site and Vicinity

W. A. Rice
Pacific Northwest Laboratory
Richland, WA 99352

Under Sandia Contract No. 37-3171

Sandia Contract Monitor
M. S. Tierney
NNWSI Repository Performance Assessments Division 6312

Abstract

Pacific Northwest Laboratory documented the data requirements, boundary conditions, and calibration of a two-dimensional, finite difference, hydrologic model of the Nevada Test Site and vicinity (southern Nevada and eastern California). Specifically, the modeled region lies between 115° and 118° west longitude, and 35° and 39° north latitude. Underflow from areas north and east of the model boundary contribute a significant flux to model input; however, water balances within the model boundary are in good agreement with published values. The major discharge flux from the model occurs along the Death Valley perimeter. If future hydraulic head data and aquifer tests were identified with hydrostratigraphic units, a two-layer, three-dimensional model could be constructed, which would more accurately simulate the physical system.

ACKNOWLEDGMENTS

The author wishes to acknowledge the efforts of several individuals who contributed to this study. The project manager, F. H. Dove, coordinated the study with our sponsor, Sandia National Laboratories, and contributed to model conceptualization. M. D. Freshley contributed to aquifer recharge calculations and document review. C. R. Cole and F. W. Bond provided technical advice regarding hydrologic modeling. P. L. Oberlander and E. A. Jacobson reviewed this document, and H. P. Foote provided the digital topography map and LANDSAT scenes that were used in the recharge calculations.

The author also wishes to acknowledge the word processing support provided by A. Jewell and the assistance with graphics provided by C. Smith.

This work, performed by Pacific Northwest Laboratory, was supported under Contract DE-AC06-76RLO 1830 with the U.S. Department of Energy. Pacific Northwest Laboratory is operated by Battelle Memorial Institute for the U.S. Department of Energy.

CONTENTS

ABSTRACT i

ACKNOWLEDGMENTS ii

INTRODUCTION 1

DESCRIPTION OF STUDY AREA 3

- CLIMATE 3
- HYDROGEOLOGY 6
- GEOCHEMISTRY 9

CONCEPTUAL MODEL 13

REGIONAL HYDROLOGIC MODEL 19

- FINITE DIFFERENCE GRID AND BOUNDARY CONDITIONS 20
- HYDRAULIC HEAD DISTRIBUTION 22
- STRUCTURAL SURFACES 25
- RECHARGE 25
- DISCHARGE 28
- TRANSMISSIVITY 31
- MODEL CALIBRATION 31
- WATER BALANCE CALCULATIONS 36

SUMMARY AND RECOMMENDATIONS 39

REFERENCES 41

APPENDIX A - DETAILED RECHARGE CALCULATION A.1

APPENDIX B - DISCHARGE CALCULATION SUMMARY TABLES B.1

APPENDIX C - CYCLIC STEADY-STATE ACTUAL EVAPOTRANSPIRTATION AND RECHARGE CALCULATION C.1

FIGURES

1 Location of Study Area 4

2 Oblique View of the Topography of the Study Area 5

3 Configuration of Flow Producing Interbasin Movement of Ground Water 14

4 Schematic Representation of the Nevada Test Site Conceptual Model 16

5 Flow Boundaries of the Regional Model 21

6 USGS-Interpreted Hydraulic Head Distribution for the Regional Model 23

7 Kriged Hydraulic Head Distribution for the Regional Model . . 24

8 Map of Kriging Error or Estimation Error for the Regional Model 26

9 Best-Estimate Annual Recharge Distribution for the Regional Model 29

10 Discharge Areas of the Regional Model 30

11 Transmissivity Distribution for the Calibrated Regional Model 32

12 Model-Predicted Hydraulic Heads for Steady-State Confined Conditions 35

TABLES

1 Stratigraphic and Hydrogeologic Units of the Study Area . . 7

2 Summary of Net Discharges with Uncertainty Bounds for the Regional Model 31

3 Comparison of Calibration Statistics for the Region Model Under Steady-State Confined Conditions 33

4 Residual Error Distribution Summary for USGS-Interpreted Hydraulic Heads and Model-Predicted Hydraulic Heads Versus Well Observations 34

5 Water Balance Summary for the Regional Model 37

INTRODUCTION

The Nevada Nuclear Waste Storage Investigations has the responsibility for determining the suitability of sites within the Nevada Research and Development Area, a small region of the Nevada Test Site (NTS), for a high-level nuclear waste repository. Pacific Northwest Laboratory (PNL) is under contract to Sandia National Laboratories to support the long-term performance assessment activities by predicting repository performance after the occurrence of selected events and processes. The predictive capability requires the use of hydrologic models that are scaled to simulate flow in unsaturated and saturated media at resolutions consistent with regional, local, and near-field applications. This report documents a preliminary two-dimensional regional hydrologic model developed for the saturated flow system surrounding Yucca Mountain.

The Department of Energy (DOE) draft siting guidelines list, as a favorable condition, the existence of hydrologic processes of the Quaternary Period that would not affect the ability of the geologic repository to isolate waste during the next 100,000 years. The regional hydrologic model provides one means of evaluating the saturated characteristics and related processes affecting repository performance. In particular, the regional hydrologic model can be used to establish the boundary conditions for a more detailed local model of the site and can be used to predict the following:

- ground-water flow paths
- ground-water discharge points
- subsurface flux
- pluvial climate effects
- man-influenced effects.

Although the repository location is expected to be a partially saturated horizon above the water table, the recharge flux entering Yucca Mountain from the surface and the distance from the repository to the water table are a function of the climate. Conservative estimates of recharge at Yucca Mountain place the modern ground-water flux at less than 10 millimeters per year (Sass and Lachenbruch 1982). The actual modern flux may be less than 1 millimeter per year (Winograd 1981). A rise in water table, possibly a result of some

future pluvial climate, could adversely affect the performance of a repository by the following:

- decreasing the distance to discharge points
- increasing subsurface flux
- decreasing the isolation capacity of the unsaturated materials.

Evidence is available to suggest that the water table observed in the carbonate system south of Yucca Mountain may have been as much as 60 meters higher in the past (Winograd and Doty 1980). The regional hydrologic model can be used to examine the implications of changing boundary conditions to produce a similar rise in regional water levels.

DESCRIPTION OF STUDY AREA

The study area considered in this report is located in southern Nevada, west of 115° 00' west longitude, and central California, east of 118° 00' west longitude (Fig. 1). The modeled region encompasses approximately 30,000 square miles of the basin and range physiographic province. The topography (Fig. 2) is characterized by isolated, elongate, block-faulted mountain ranges and broad, intervening, nearly flat alluvial valleys or basins. The mountains trend north to northeast and have elevations between 8,000 and 11,000 feet above mean sea level (MSL). The basins and valleys are filled with varying degrees of thickness of alluvium derived from the surrounding mountains. Valley floor elevations range from below sea level in Death Valley to 5,000 feet in the northern part of the study area.

CLIMATE

The climate is arid to semiarid, characterized by short, mild winters with light snow in the mountains and long, hot, dry summers. The mean daily maximum temperatures at Las Vegas range from 13.0°C in January to 40.5°C in July; the mean daily minimum for the same months ranges from 0.5°C to 24.5°C. In Death Valley, located in the southwest part of the study area, temperatures greater than 49.0°C are common during summer months (Winograd and Thordarson 1975).

Precipitation is a function of elevation and ranges from less than 3 inches in some of the southern valleys and basins to more than 30 inches per year in the highest mountains. The majority of basins and foothills receive 5 to 12 inches of annual rainfall. The winter moisture that accumulates in the mountains and is stored in snowpacks constitutes the most effective form of precipitation for recharge to the ground-water system. Intense and localized thunderstorms that occur during warmer months can generate flash floods in dry washes where runoff reaches surface water sinks (i.e., playas), and part of it is lost to the ground-water system in transit. Pan evaporation, which is between 5 and 25 times the annual rainfall, precludes rainfall infiltration to the ground water, except during these sudden storms (Hunt et al. 1966).

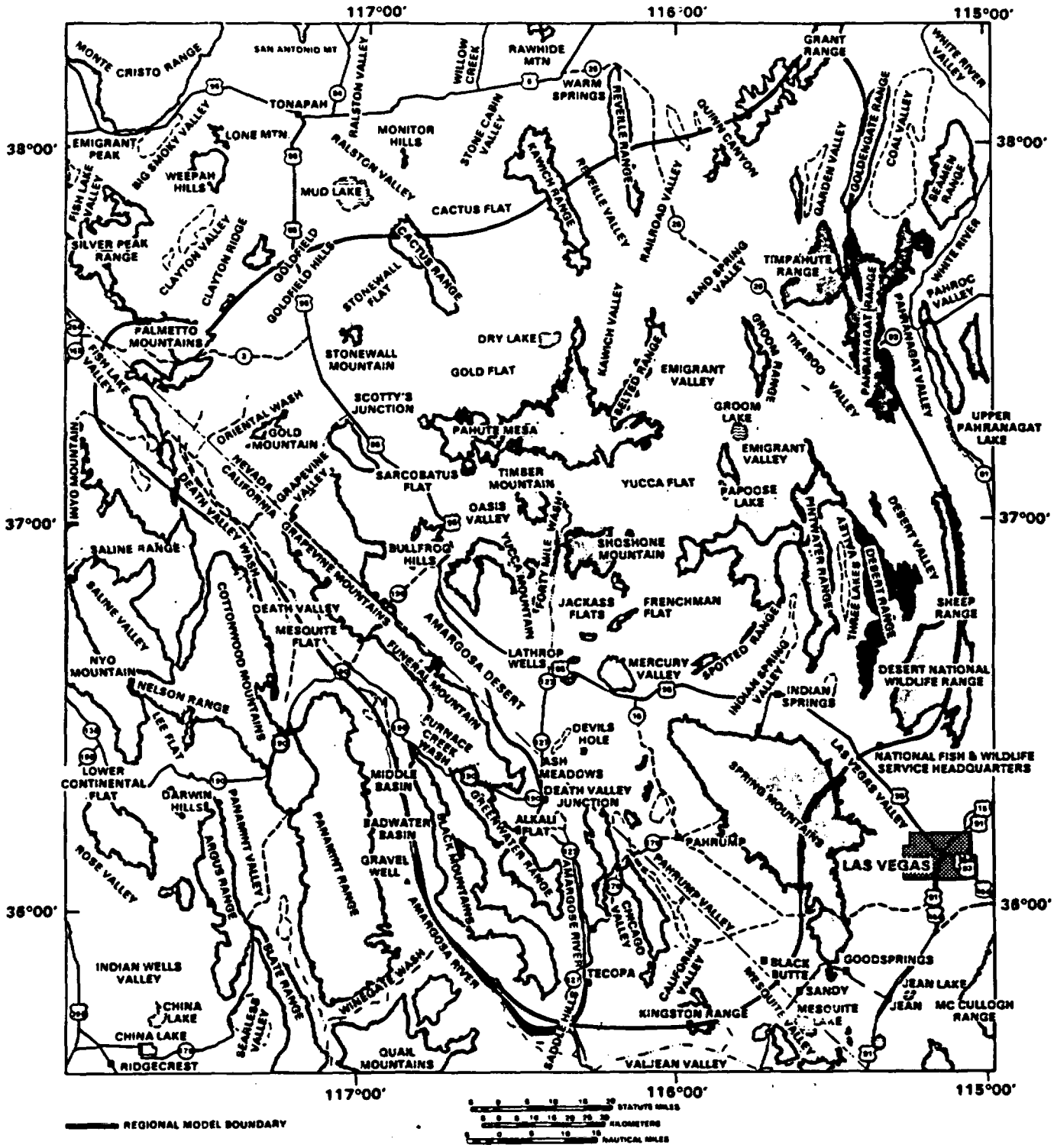

FIGURE 1. Location of Study Area

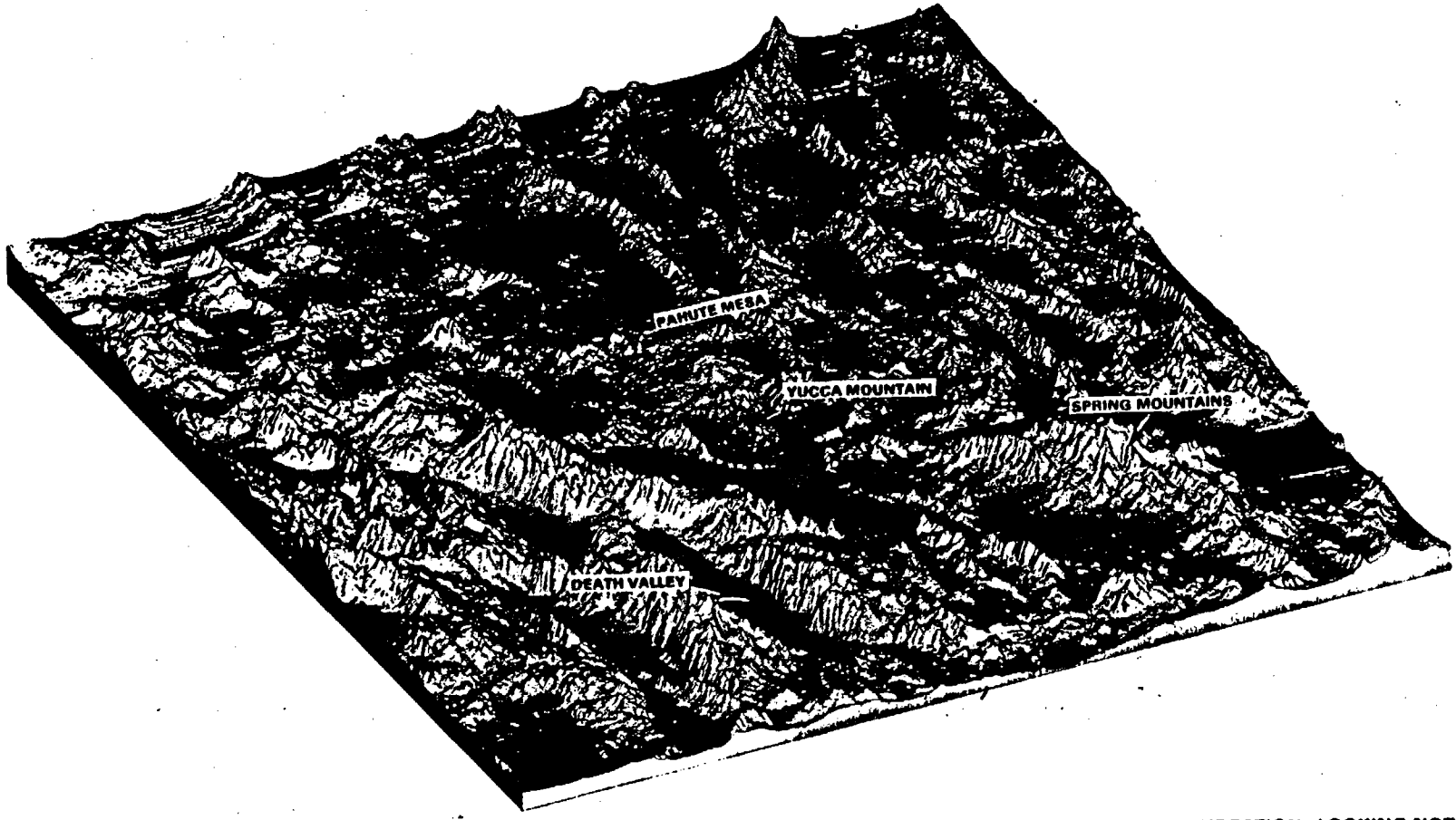

VIEWING DIRECTION: LOOKING NORTHEAST
REGION: 185 MI N-S BY 160 MI E-W
PLOT CENTER: LONG 116° LAT. 37°
VERTICAL EXAGGERATION: 6
DATA SOURCE: DMA TOPOGRAPHIC FILES

FIGURE 2. Oblique View of the Topography of the Study Area

HYDROGEOLOGY

The stratigraphy and structure of the NTS and surrounding region are complex, reflecting extensive Precambrian and Paleozoic sedimentation, Mesozoic folding and thrust faulting, and Cenozoic volcanism and block faulting. Table 1 lists the major rock types found in the study area, their stratigraphic relationship, and their hydrologic properties.

The oldest sedimentary rocks in the study area are sometimes termed the lower clastic aquitard and are comprised of low permeable sandstones and shales that range in age from Precambrian to Cambrian. Overlying these rocks are highly permeable limestones and dolomites, which outcrop in the southern and eastern part of the study area and range in age from Cambrian to Devonian. Winograd and Thordarson (1975) called these limestones and dolomites the lower carbonate aquifer. It plays a significant role in the regional flow system in the study area. The term upper clastic aquitard was used by Winograd and Thordarson (1975) to categorize the assemblage of the less permeable rocks of the Eleana Formation, which overlie the lower carbonate aquifer. Overlying this aquitard is a thick sequence of tertiary tuffs originating from eruption centers in the western part of the modeled area. These volcanic rocks are generally less permeable than the lower carbonate aquifer, but can locally be highly permeable when fractured. The most recent sequence is the valley-fill aquifer or alluvium, which is composed of unconsolidated alluvial, colluvial, and lacustrine deposits. The alluvium is located in the valleys or basins of the study area and is generally in hydrologic connection with the carbonate or volcanic aquifers.

Geologic structure has affected the regional hydrology of this region by 1) large-scale folding and block faulting, which have formed the major topographic features and sedimentary basins; 2) faulting and intense folding, which have fractured the hard limestones and dolomites creating highly permeable channels in the lower carbonate aquifer; and 3) faulting and folding, which have created barriers to water movement and the emergence of springs.

TABLE 1. Stratigraphic and Hydrogeologic Units of the Study Area[a]

System	Series	Stratigraphic unit	Major lithology	Maximum thickness (feet)	Hydrogeologic unit	Water-bearing characteristics and extent of saturation
Quaternary and Tertiary	Holocene, Pleistocene, and Pliocene	Valley fill	Alluvial fan, fluvial, fanglomerate, lakebed, and mudflow deposits	2,000	Valley-fill aquifer	Coefficient of transmissibility ranges from 1,000 to 35,000 gpd per ft; average coefficient of interstitial permeability ranges from 5 to 70 gpd per sq ft; saturated only beneath structurally deepest parts of Yucca Flat and Frenchman Flat.
Tertiary	Pliocene	Basalt of Kiwi Mesa	Basalt flows, dense and vesicular.	250	Lava-flow aquifer	Water movement controlled by primary (cooling) and secondary fractures and possibly by rubble between flows; intercrystalline porosity and permeability negligible; estimated coefficient of transmissibility ranges from 500 to 10,000 gpd per ft; saturated only beneath east-central Jackass Flats.
		Rhyolite of Shoshone Mountain	Rhyolite flows.	2,000		
		Basalt of Skull Mountain	Basalt flows.	250		
		Piapi Canyon Group, Timber Mountain Tuff: Ammonia Tanks Member	Ash-flow tuff, moderately to densely welded; thin ash-fall tuff at base.	250	Welded-tuff aquifer	Water movement controlled by primary (cooling) and secondary joints in densely welded part of ash-flow tuff; coefficient of transmissibility ranges from 100 to 100,000 gpd per ft; intercrystalline porosity and permeability negligible; unwelded part of ash-flow tuff, where present, has relatively high interstitial porosity (35–50 percent) and modest permeability (2 gpd per sq ft) and may act as leaky aquitard; saturated only beneath structurally deepest parts of Yucca, Frenchman, and Jackass Flats.
		Rainier Mesa Member	Ash-flow tuff, nonwelded to densely welded; thin ash-fall tuff at base.	600		
	Miocene	Piapi Canyon Group, Paintbrush Tuff: Tiva Canyon Member	Ash-flow tuff, nonwelded to densely welded; thin ash-fall tuff near base.	300–360		
		Topopah Spring Member	Ash-flow tuff, nonwelded to densely welded; thin ash-fall tuff near base.	890		
		Bedded tuff (informal unit)	Ash-fall tuff and fluvially reworked tuff.	1,000	Bedded-tuff aquifer	Coefficient of transmissibility ranges from 200 to 1,000 gpd per ft; saturated only beneath structurally deepest parts of Yucca Flat, Frenchman Flat, and Jackass Flats; Occurs locally below ash-flow tuff members of Paintbrush Tuff and below Grouse Canyon Member of Indian Trail Formation.
		Wahmonie Formation	Lava-flow and interflow tuff and breccia; locally hydrothermally altered.	4,000	Lava-flow aquitard	Water movement controlled by poorly connected fractures; interstitial porosity and permeability negligible; coefficient of transmissibility estimated less than 800 gpd per ft; contains minor perched water in foothills between Frenchman Flat and Jackass Flats.
			Ash-fall tuff, tuffaceous sandstone, and tuff breccia, all interbedded; matrix commonly clayey or zeolitic.	1,700	Tuff aquitard	Coefficient of transmissibility ranges from 100 to 200 gpd per ft; interstitial porosity is as high as 40 percent, but interstitial permeability is negligible (6×10^{-7} to 6×10^{-9} gpd per sq ft); owing to poor hydraulic connection of fractures, interstitial permeability probably controls regional ground-water movement; perches minor quantities of water beneath foothills flanking valleys; fully saturated only beneath structurally deepest parts of Yucca Flat, Frenchman Flat, and Jackass Flats; Grouse Canyon and Tub Spring Members of Indian Trail Formation may locally be aquifers in northern Yucca Flat.
		Salyer Formation	Breccia flow, lithic breccia, and tuff breccia, interbedded with ash-fall tuff, sandstone, siltstone, claystone, matrix commonly clayey or calcareous.	2,000		
		(?)				
		Indian Trail Formation: Grouse Canyon Member	Ash-flow tuff, densely welded.	200		
		Tub Spring Member.	Ash-flow tuff, nonwelded to welded.	300		
		Local informal units	Ash-fall tuff, nonwelded to semiwelded ash-flow tuff, tuffaceous sandstone, siltstone, and claystone; all massively altered to zeolite or clay minerals; locally, minor welded tuff near base; minor rhyolite and basalt.	2,000		
		(?)				
		Rhyolite flows and tuffaceous beds of Calico Hills	Rhyolite, nonwelded and welded ash flow, ash-fall tuff, tuff breccia, tuffaceous sandstone; hydrothermally altered at Calico Hills; matrix of tuff and sandstone commonly clayey or zeolitic.	>2,000		
	Miocene and Oligocene	Tuff of Crater Flat	Ash-flow tuff, nonwelded to partly welded, interbedded with ash-fall tuff; matrix commonly clayey or zeolitic.	300		
		Rocks of Pavits Spring	Tuffaceous sandstone and siltstone, claystone; fresh-water limestone and conglomerate; minor gypsum; matrix commonly clayey, zeolitic, or calcareous.	1,400		
	Oligocene	Horse Spring Formation	Fresh-water limestone, conglomerate, tuff.	1,000		

(a) After Winograd and Thordarson (1975).

TABLE 1. (contd)

System	Series	Stratigraphic unit	Major lithology	Maximum thickness (feet)	Hydrogeologic unit	Water-bearing characteristics and extent of saturation[1]
Cretaceous to Permian		Granitic stocks	Granodiorite and quartz monzonite in stocks, dikes, and sills.		(A minor aquitard)	Complexly fractured but nearly impermeable.
Permian and Pennsylvanian		Tippipah Limestone	Limestone.	3,600	Upper carbonate aquifer	Complexly fractured aquifer; coefficient of transmissibility estimated in range from 1,000 to 100,000 gpd per ft; intercrystalline porosity and permeability negligible; saturated only beneath western one-third of Yucca Flat.
Mississippian and Devonian		Eleana Formation	Argillite, quartzite, conglomerate, conglomerite, limestone.	7,900	Upper clastic aquitard	Complexly fractured but nearly impermeable; coefficient of transmissibility estimated less than 500 gpd per ft; interstitial permeability negligible but owing to poor hydraulic connection of fractures probably controls ground-water movement; saturated only beneath western Yucca Flat and Jackass Flats.
Devonian	Upper	Devils Gate Limestone	Limestone, dolomite, minor quartzite.	>1,380	Lower carbonate aquifer	Complexly fractured aquifer which supplies major springs throughout eastern Nevada; coefficient of transmissibility ranges from 1,000 to 1,000,000 gpd per ft; intercrystalline porosity and permeability negligible; solution caverns are present locally but regional ground-water movement is controlled by fracture transmissibility; saturated beneath much of study area.
	?					
	Middle	Nevada Formation	Dolomite.	>1,525		
Devonian and Silurian		Undifferentiated	Dolomite.	1,415		
Ordovician	Upper	Ely Springs Dolomite	Dolomite.	305		
	Middle	Eureka Quartzite	Quartzite, minor limestone.	340		
	?	Pogonip Group: Antelope Valley Limestone	Limestone and silty limestone.	1,530		
	Lower	Pogonip Group: Ninemile Formation	Claystone and limestone, interbedded.	335		
		Pogonip Group: Goodwin Limestone	Limestone.	>900		
Cambrian	Upper	Nopah Formation: Smoky Member	Dolomite, limestone.	1,070		
		Nopah Formation: Halfpint Member	Limestone, dolomite, silty limestone.	715		
		Dunderberg Shale Member	Shale, minor limestone.	225		
	Middle	Bonanza King Formation: Banded Mountain Member	Limestone, dolomite, minor siltstone.	2,440		
		Bonanza King Formation: Papoose Lake Member	Limestone, dolomite, minor siltstone.	2,160		
		Carrara Formation	Siltstone, limestone, interbedded. Upper 1,050 feet predominantly limestone; lower 950 feet predominantly siltstone.	1,050		
				950	Lower clastic aquitard[2]	Complexly fractured but nearly impermeable; supplies no major springs; coefficient of transmissibility less than 1,000 gpd per ft; interstitial porosity and permeability is negligible, but probably controls regional ground-water movement owing to poor hydraulic connection of fractures; saturated beneath most of study area.
	Lower	Zabriskie Quartzite	Quartzite.	220		
		Wood Canyon Formation	Quartzite, siltstone, shale, minor dolomite.	2,285		
Precambrian		Stirling Quartzite	Quartzite, siltstone.	3,400		
		Johnnie Formation	Quartzite, sandstone, siltstone, minor limestone and dolomite.	3,200		

[1]Coefficient of transmissibility has the units gallons per day per foot (gpd per ft) width of aquifer; coefficient of permeability has the units gallons per day per square foot (gpd per sq ft) of aquifer.

[2]The three Miocene sequences occur in separate parts of the region. Age correlations between them are uncertain. They are placed vertically in table to save space.

[3]The Noondaya(?) Dolomite, which underlies the Johnnie Formation, is considered part of the lower clastic aquitard.

GEOCHEMISTRY

Water from wells within this study area was chemically analyzed to 1) define the boundary of regional ground-water basins, 2) determine the direction of flow within these basins, and 3) estimate the amount of downward leakage of water from the Cenozoic volcanic rocks into the lower carbonate aquifer. The regional geochemistry presented here follows Winograd and Thordarson (1975) and Winograd (1971). These authors relied on previous chemical studies presented in Clebsch and Barker (1960), Malmberg and Eakin (1962), Maxey and Jameson (1948), Moore (1961), Pistrang and Kunkel (1964), Schoff and Moore (1964), and Walker and Eakin (1963).

Schoff and Moore (1964) recognized three types of ground water at the NTS and its vicinity based on chemical analyses: 1) sodium and potassium bicarbonate water, 2) calcium and magnesium bicarbonate water, and 3) mixed water. The sodium and potassium bicarbonate water is found in the tuff aquifers and aquitards, and in valley-fill aquifers of Emigrant Valley, Yucca Flat, Fenchman Flat, and Jackass Flats. The calcium and magnesium bicarbonate water is found in the Paleozoic carbonate aquifers as well as in the valley-fill aquifer in southern Indian Springs Valley, which is rich in carbonate-rock detritus. The mixed waters have characteristics of both preceding types and are presumed to have been formed in one of three ways: 1) movement of water from tuffaceous into carbonate rocks (or alluvium with carbonate rock detritus), followed by dissolution of carbonate minerals; 2) movement of water from carbonate rocks into tuff (or tuffaceous alluvium), followed by aquisition of sodium either by solution or by ion exchange of calcium for sodium; or 3) mixing of calcium and magnesium bicarbonate water with sodium and potassium bicarbonate water. The mixed water occurs in the lower carbonate rocks found predominately in the Amargosa Desert.

Major inferences pertinent to delineation of regional ground-water basins and the movement of ground water within those basins are summarized here. First, analysis of the sodium content (Schoff and Moore 1964) reveals that ground water in the carbonate rocks beneath the NTS and vicinity moves toward the Ash Meadows Spring discharge zone in the Amargosa Desert where there is

generally a mixed-type ground water of higher sodium and dissolved solids than that found in southern Indian Springs Valley. This rules out the possibility of ground-water movement from the Nevada Test Site to Indian Springs Valley.

Second, the chemical quality of water within the lower carbonate aquifer may not change markedly with depth. Analyses of chemical data from four wells at NTS, three deep oil test wells in east-central Nevada, and the chemical content of Ash Meadows discharges indicate no significant increase in the dissolved solids content in the lower carbonate aquifer to depths of several thousand feet.

Third, Schoff and Moore (1964) conclude that water in the Paleozoic carbonate rocks underlying the NTS is recharged by percolation downward through the tuff or alluvium containing detrital tuff, which results in mixed-type water. The differences in the chemical quality of waters in the tuff and carbonate aquifers have been used in a mass balance relationship quantifying the recharge from the tuffs to the lower carbonate aquifer as probably less than 5% of the Ash Meadows discharge.

Fourth, postulated underflow from Pahranagat Valley into the Ash Meadows ground-water basin is compatible with geochemical data. Comparison of deuterium content of ground water in Pahranagat Valley, along the flanks of Spring Mountain, and at Ash Meadows indicates that as much as 35% of the Ash Meadows discharge may originate in Pahranagat Valley (and possibly Garden and Coal Valleys).

Fifth, the ground-water movement from Pahrump and Stewart Valleys into Ash Meadows is small. This conclusion is based on the relatively higher dissolved solids, chloride, sulfate, potassium, and sodium content of Ash Meadows waters compared to ground water in the Pahrump Valley, which is recharged primarily on the upper slopes of Spring Mountain. Extensive outcrops of carbonate rocks on Spring Mountain cause ground water to be of the calcium and magnesium bicarbonate-type rather than the mixed-type found at Ash Meadows.

Sixth, the flow from the central Amargosa Desert into Death Valley is the most likely source of major spring discharge in east-central Death Valley.

Ground water in Death Valley may be a mixture from Oasis Valley and Ash Meadows. On the basis of chemical analysis, spring discharge at the Furnace Creek Wash-Nevares Spring area seems to originate from water in the valley-fill aquifer in central and northwestern Amargosa Desert.

CONCEPTUAL MODEL

The fundamental concepts of flow systems in the study area have been investigated by Eakin (1966), Eakin et al. (1951), Eakin and Moore (1964), Eakin and Winograd (1965), Grove et al. (1969), Hunt and Robinson (1960), Loeltz (1960), Maxey (1968), Maxey and Mifflin (1966), Miller (1977), Pistrang and Kunkel (1964), Walker and Eakin (1963), Winograd (1962; 1971) Winograd and Friedman (1972), and Winograd and Thordarson (1975). These researchers report that generally two ground-water systems are found in the study area, a 'regional' and 'local' system, which are defined as follows:

- A 'regional' ground-water flow system is loosely defined as a large ground-water flow system that encompasses one or more topographic basins.
  - Regional systems may include several ground-water basins.
  - Interbasin flow is common and important with respect to the total volume of water transferred within the system boundaries.
  - Lengths of flow paths are relatively long when compared to lengths of flow paths of 'local' ground-water flow systems.
- A 'local' ground-water flow system is generally confined to one topographic or ground-water basin.
  - Interbasin flow is not important with respect to total volume of water transferred within the system.
  - The majority of water flow in the system discharges within the associated ground-water basin.
  - Flow paths are relatively short when compared to those in regional systems.

Freeze and Witherspoon (1966; 1967) have studied regional flow systems and found that flows of large quantities can occur at depths if a zone of relatively high permeability exists as illustrated in Figure 3. They have determined the following general characteristics of regional flow systems: 1) ground-water discharge tends to be concentrated in major valleys,

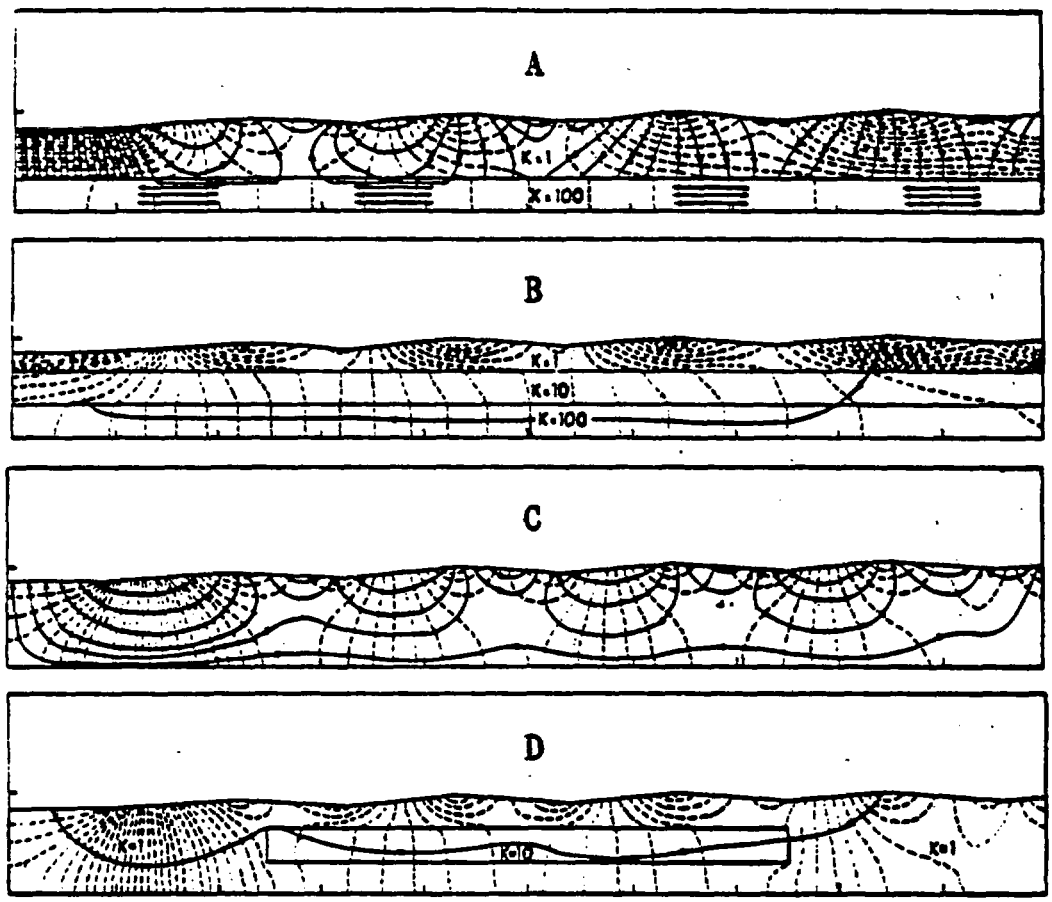

A and B - Situation of interbasin flow produced by greater relative permeability at depth and relief.

C - Situation of interbasin flow produced by relief alone, in uniform permeability media.

D - Situation of interbasin flow created by lense of permeability material.

← - Flow line

—— - Equipotential line

K - Relative Hydraulic Conductivity

FIGURE 3. Configuration of Flow Producing Interbasin Movement of Ground Water (modified after Freeze and Witherspoon 1967)

2) recharge areas are larger than discharge areas, 3) many subbasins are superposed on a regional flow system in a hammocky terrain, 4) buried aquifers tend to direct flow toward the principal discharge area with little or no effect on the subbasins and can produce artesian conditions, and 5) geologic structures can distribute recharge and discharge independently of the configuration of the water table.

All five of the preceding conditions exist in the study area. There are local flow systems that sit in a hammocklike fashion in the numerous intermontane valleys and basins as in Figure 2. These systems constitute the valley-fill aquifer and are composed of alluvial material. Underlying these local systems is a massive interbasin or regional flow system composed of highly fractured carbonate rock that is an avenue of flow beneath the local systems. The regional system is confined in the deepest portions of the valleys and unconfined beneath the mountain ridges.

The most compelling evidence for the existence of the regional flow system is from the recharge versus discharge estimates for the local subbasins made during the 1960s and 1970s by the Nevada Department of Conservation and Natural Resources, and reported in the State of Nevada Ground Water Reconnaissance Series and Water Resources Bulletins. In many valleys these water budgets were impossible to balance because the accountable discharges were several times less than the recharge estimated from precipitation alone. Because the differences were significantly larger than the errors in the inflow estimates, the general conclusion by personnel (Eakin 1966) at the U.S. Geological Survey (USGS) and Maxey and Mifflin (1966) at the Desert Research Institute, Reno, Nevada, was that while the valleys are topographically separated, ground-water flow is significant between the subbasins in the region. This interbasin ground-water flow occurred primarily where a significant portion of the geologic cross section was carbonate rock. The occurrence of springs issuing from or near fractured carbonate rocks and the regional ground-water chemistry (see previous section) also supports the existence of a regional flow system.

Thus, the conceptual model presented in Figure 4 was developed so that the highly permeable sequence of carbonate rock, termed the carbonate aquifer

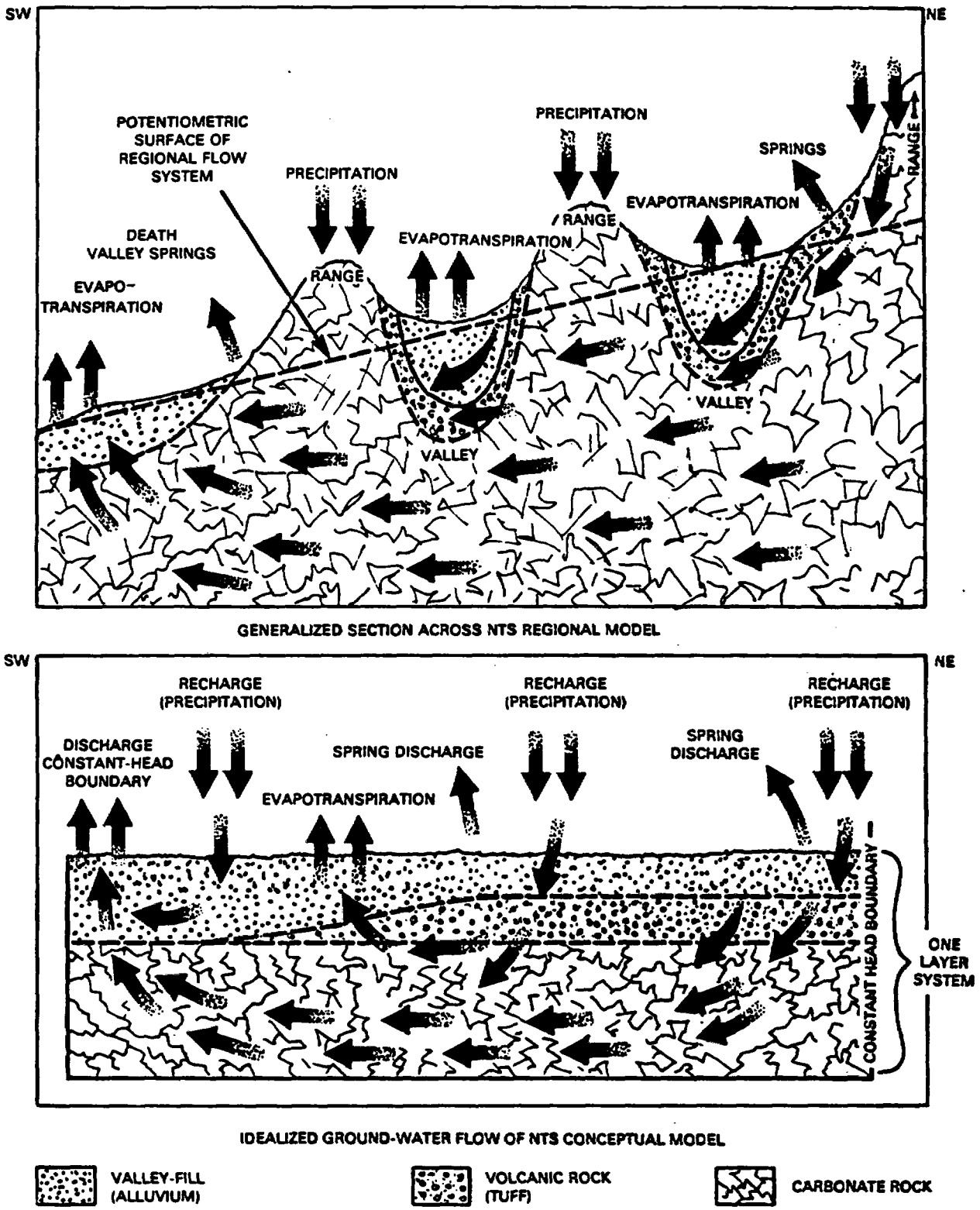

FIGURE 4. Schematic Representation of the Nevada Test Site Conceptual Model

by Winograd and Thordarson (1975), is primarily responsible for interbasin or regional ground-water flow. Recharge occurs in the mountainous areas at higher elevations where more precipitation occurs and pan evaporation is less. Water can directly recharge the lower carbonate aquifer where it is exposed in mountainous areas, or it can move downward through the alluvium and volcanic tuffs to recharge the carbonate aquifer. Ground water then moves laterally in this unit toward discharge areas occurring primarily in the valleys in the form of springs, evapotranspiration, and pumping. The schematic representation of the conceptual model in Figure 4 considers the multilayered flow system composed of the alluvial, volcanic, and carbonate aquifers as one unit. At a particular location, the model simulates the most transmissive hydrostratigraphic unit(s).

Several simplifying assumptions regarding the hydrogeology of the study area were made primarily because of lack of data in order to develop the conceptual model:

1. Ground-water flow is strictly horizontal. Evidence exists for both upward and downward flow beneath Pahute Mesa (Blankennagel and Weir 1973; Oberlander 1979). Although no data are available on vertical head distributions in most areas, geometric considerations suggest that flow beneath recharge areas is downward, and flow beneath discharge areas is upward (see Fig. 4). It was not possible to construct a three-dimensional, multilayered model to simulate vertical flow in these areas because the hydraulic head data available were composite heads that were not keyed to specific hydrostratigraphic units.

2. Hydrologic parameters (transmissivity, rates of recharge and discharge) do not change with time, and the current hydraulic head distribution is assumed to be at steady state. The steady-state assumption is known to be violated by natural flow systems because several processes are currently taking place that are known to change the system characteristics with time. For example, in areas where pumping has been intense (Ash Meadows, and Pahrump and Sand Spring Valleys) there are short-term changes in water levels. These changes have been documented and appear to be small compared to the range of hydraulic heads throughout the study

area and the uncertainty in the interpreted hydraulic head distribution. Also, the occurrence of pluvial climatic conditions could significantly change the present water table elevations in the study area.

3. The aquifers are assumed to be isotropic with respect to transmissivity. Few porous media are isotropic (Freeze and Cherry 1979) and the assumption does not apply to this study area. The effects of applying this assumption are 1) transmissivity calculated or used in the model is representative of transmissivity in the direction of flow and 2) errors will result from calculations of fluxes and flow directions because the flow occurs perpendicular to the hydraulic head contours unless translated by a transmissivity or hydraulic conductivity tensor.

4. For the preliminary modeling activities discussed in this report, the flow system is modeled under confined conditions, and the surface recharge is allowed to infiltrate directly to the confined aquifer.

REGIONAL HYDROLOGIC MODEL

Various hydrologic codes exist at PNL that are capable of assessing simple to complex flow conditions. After considering the conceptual model, the amount of data available, and conditions existing in the regional flow system of this study area, the two-dimensional Variable Thickness Transient (VTT) code described by Reisenauer (1980) was selected as appropriate. This code uses a finite difference formulation to represent the partial differential flow equation with numerical expressions. Specifically, a horizontal x-y coordinate grid is adopted over the study area. Model parameters are then assigned to and evaluated at the center of each grid block or node and are considered representative of the whole grid block area. From the assigned parameters, the model solves for the hydraulic head for each node.

The parameters defining the aquifer systems that must be assigned to each node (where the units are L for length and T for time) for steady-state conditions are listed below:

- elevation of the land surface (L above mean sea level)
- elevation of top of the regional aquifer for confined systems (L above mean sea level)
- elevation of the bottom of the aquifer (L above mean sea level)
- initial ground-water surface elevation (hydraulic head) of the aquifer (L above mean sea level)
- transmissivity (L^2/T) or hydraulic conductivity (L/T) of the aquifer
- recharge (L^3/T) to the aquifer
- discharge (or pumping) rate (L^3/T) from the aquifer.

Following the formulation of the conceptual model, the next step is to implement the conceptual model via the VTT hydrologic flow code by the following:

- determining the boundary conditions for the modeled region

- interpreting and refining the published or unpublished data for input to the model
- using the data to calibrate the model
- applying the model to predict quantity of water flowing into or out of the regional flow system.

Each portion of the above sequence is discussed in more detail below.

FINITE DIFFERENCE GRID AND BOUNDARY CONDITIONS

The regional hydrologic model area as defined by the VTT code was divided into a 70 by 80 node grid, with each node 2.367 mile (12,500 feet) on a side. The grid registers between 114° 59' and 117° 54' west longitude and 35° 34' and 38° 19' north latitude. The regional system was modeled as a one-layer flow system combining valley-fill (alluvium), volcanic (tuff), and carbonate aquifers in a single unit. Figure 5 shows the flow boundaries of the hydrologic model. These boundaries were established along the following topographic highs: on the north--the Palmetto Mountains, Catus, Kawich, Reveille and Grant Ranges; on the east--Pahranagat Range, Sheep Range, and Spring Mountain; and on the south--Kingston Range and Saddle Hills. Death Valley, a topographic low, defines the western discharging boundary of the hydrologic model. The major discharging boundary, Death Valley, and the major recharging boundaries (the north and east boundary), were held at the water table elevations of a hand-contoured hydraulic head map provided by the Denver Office of the USGS.

Most regional models constructed at PNL extend out to no-flow boundary conditions. Caution, however, must be used when applying the term 'no flow' to this study area. The limited hydraulic head data and the interbasin movement of ground water through the potentially thick, extensive lower carbonate aquifer, preclude the routine use of topographic divides to define the boundaries of the ground-water basins in this study area. For example, Eakin (1966) suggests that geology may control in part the southwesterly movement of water from southern Pahranagat Valley into Desert Valley and thus, across the hydrologic boundary established for this model. Geochemical

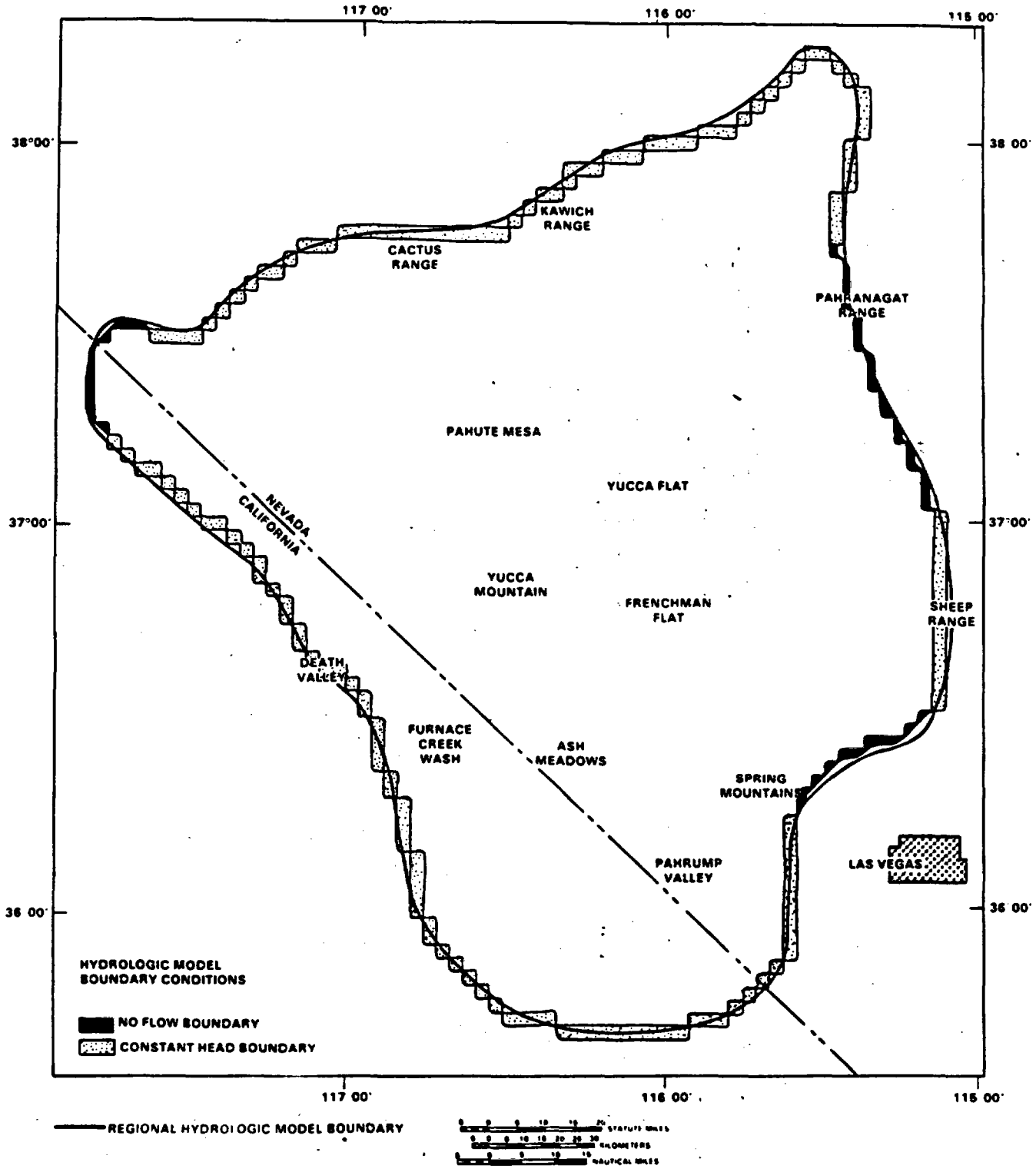

FIGURE 5. Flow Boundaries of the Regional Model

evidence presented by Winograd and Thordarson (1975) and the results of this hydrologic modeling effort indicate that ground water from Pahranagat as well as Garden and Coal Valleys contributes to the discharge at Ash Meadows. Also the relationship of ground-water flow in Pahrump and Stewart Valleys to ground-water flow in the Ash Meadows basin is not clear. Winograd (1971) believes that only 4% of the flow of these two valleys contributes to Ash Meadows discharge. Most of the flow exiting Pahrump Valley is underflow to the south and west indicating that ground-water flow in Pahrump Valley is relatively independent of the Ash Meadows ground-water basin.

HYDRAULIC HEAD DISTRIBUTION

Two hydraulic head distributions were considered in this study. The first distribution is a hand-contoured ground-water elevation map interpreted by the Denver Office of the USGS and transferred to PNL on March 31, 1982. This distribution will be referred to as the USGS-interpreted hydraulic head distribution. Figure 6 shows the digitized version of the USGS-interpreted head hydraulic distribution after it has been interpolated to the nodal system of the hydrologic model. Figure 6 also provides the well locations and a corresponding water table measurement at each well, which were used by the USGS in contouring this hydraulic head distribution.

Pacific Northwest Laboratory also used a geostatistical technique, universal kriging (Devary and Rice 1983), to calculate a statistically unbiased hydraulic head distribution that optimally fits the 240 water table measurements shown in Figure 6. The kriged hydraulic head distribution shown in Figure 7 was calculated using a zero-order drift and the covariance function: $K|h| = 0.08 - 1.5459|h|$. The similarity in shape between the USGS-interpreted and the kriged hydraulic head distributions is evident if Figures 6 and 7 are compared.

Uncertainty in the Hydraulic Head Distribution

The uncertainty in the USGS-interpreted hydraulic head distribution was determined by comparing the USGS hand-contoured distribution with water table measurements at well locations. The average and root-mean-squared error difference between the USGS-interpreted distribution and well data is 23.7 and 34.3 meters, respectively.

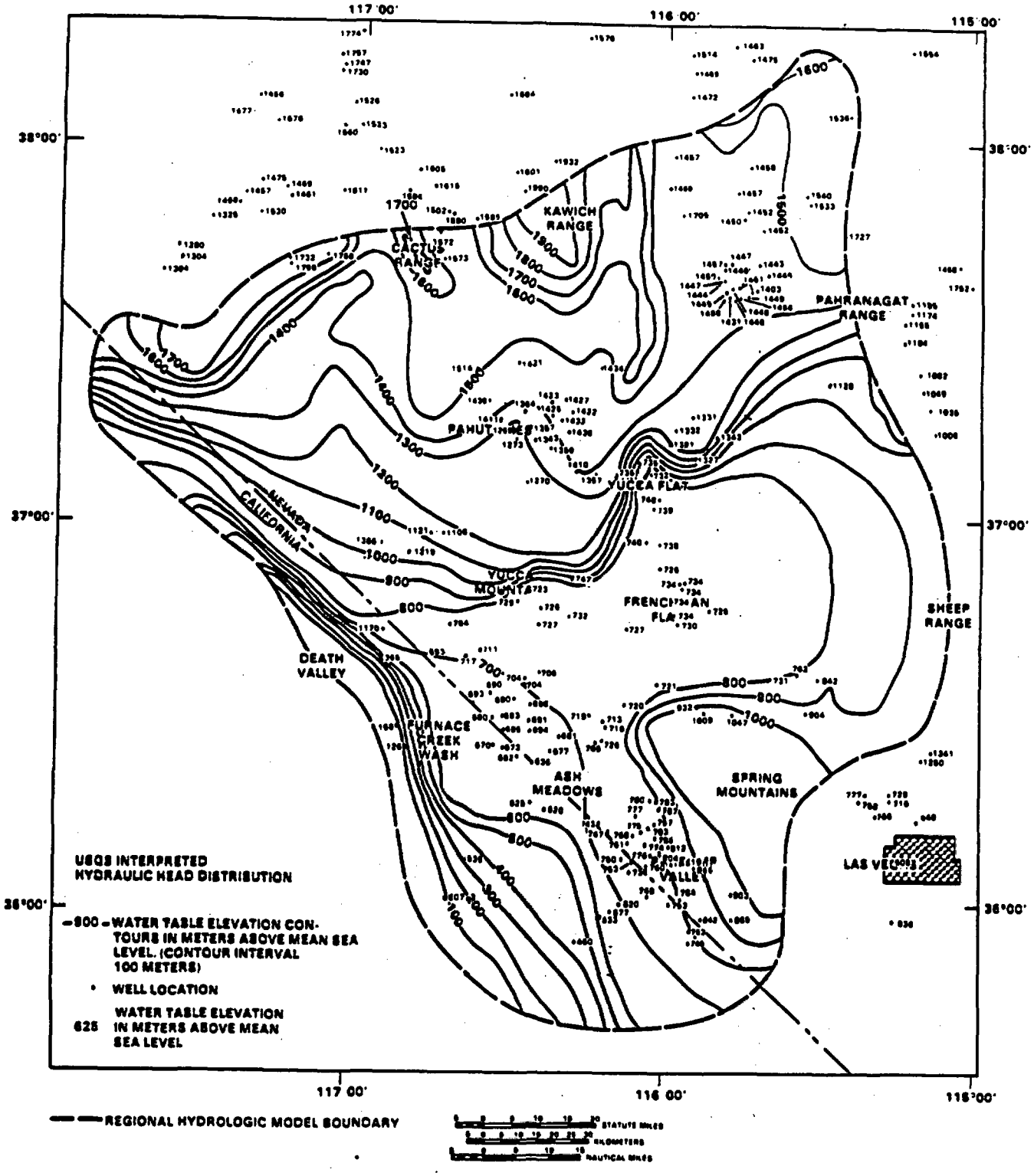

FIGURE 6. USGS-Interpreted Hydraulic Head Distribution for the Regional Model (hydraulic heads in meters above MSL)

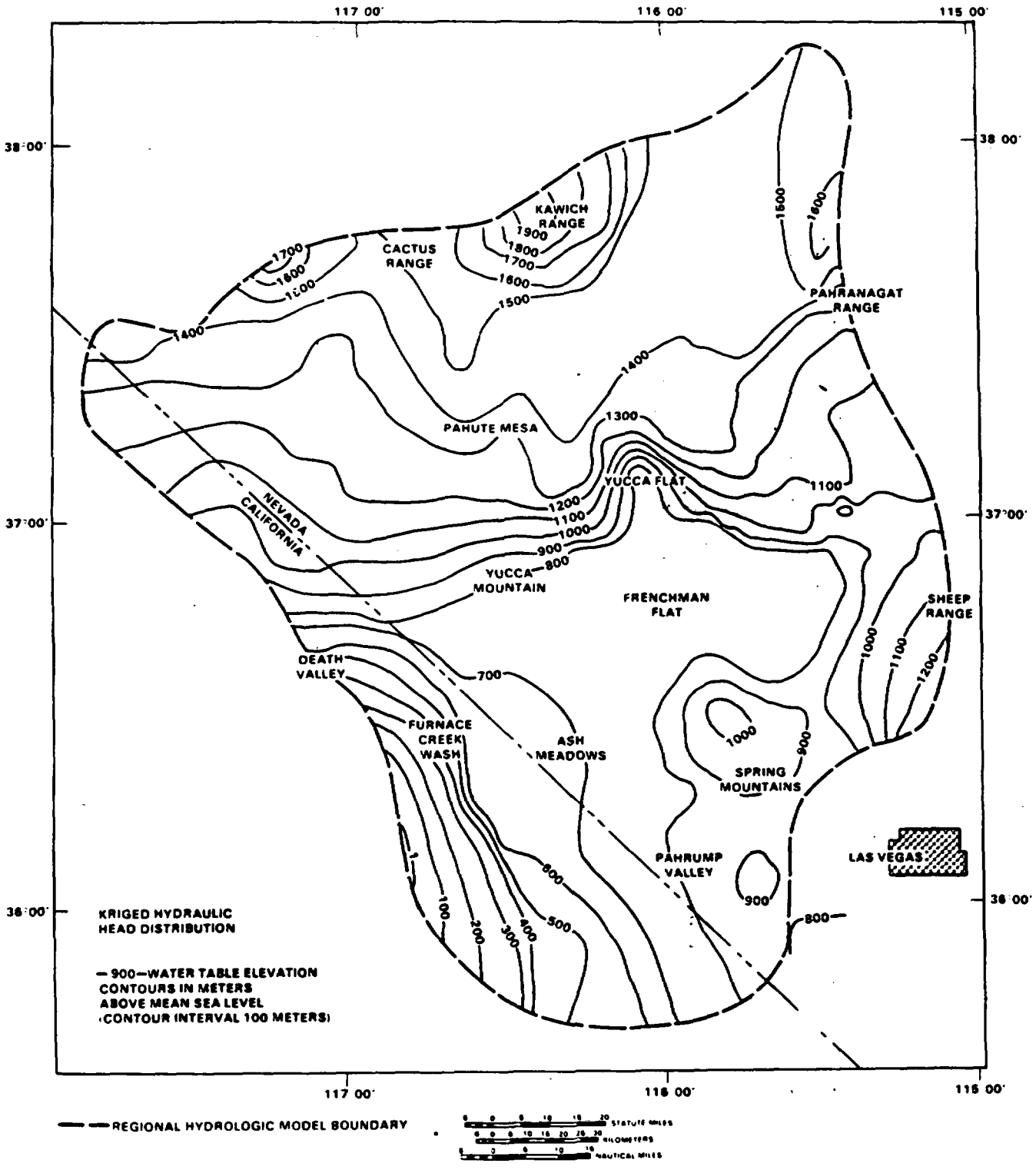

FIGURE 7. Kriged Hydraulic Head Distribution for the Regional Model (hydraulic heads in meters above MSL)

The kriging error provides a second measure of the uncertainty in the hydraulic head distribution. The kriging or estimation error is the standard deviation (square root of the variance) of each estimated point. Figure 8 is a contour map of the kriging error. Areas of greatest error occur in mountainous regions where well data are most deficient; here the hydraulic head may be in error more than 100 meters. Note that the mountainous regions are also the major recharging areas for the hydrologic model. Where farming activity has increased the number of wells as in Pahrump Valley, Sand Spring Valley, and the Amargosa Desert, the hydraulic head error is reduced to 30 meters. The regional hydraulic head uncertainty near Yucca Mountain exhibits an intermediate error between 25 and 75 meters. The average kriging error considering all nodes within the boundaries of the hydrologic model is 87.6 meters.

STRUCTURAL SURFACES

Structural surfaces (aquifer top and bottom) for the regional model were not used because the few wells drilled deep enough to penetrate the carbonate aquifer, rarely penetrate its full saturated thickness. Consequently, the base definition of the regional aquifer is poor. Instead, transmissivity is used in the hydrologic model (transmissivity = hydraulic conductivity x saturated thickness) eliminating the need for structural surfaces. Since the purpose of this hydrologic model is to determine flux, the use of transmissivity does not present a problem.

RECHARGE

Precipitation in the topographically high regions is the major source of recharge into the regional ground-water system. Lesser amounts of recharge occur through recycled irrigation and domestic waters, as well as seepage of spring discharge back into the ground-water system. The recharge calculation used in this model accounts for recharge due to precipitation alone. Irrigation, recycled domestic waters, and seepage of spring waters that originate in the ground water, are handled as a net discharge (i.e., discharge minus recycled water) and are discussed in the section on discharge.

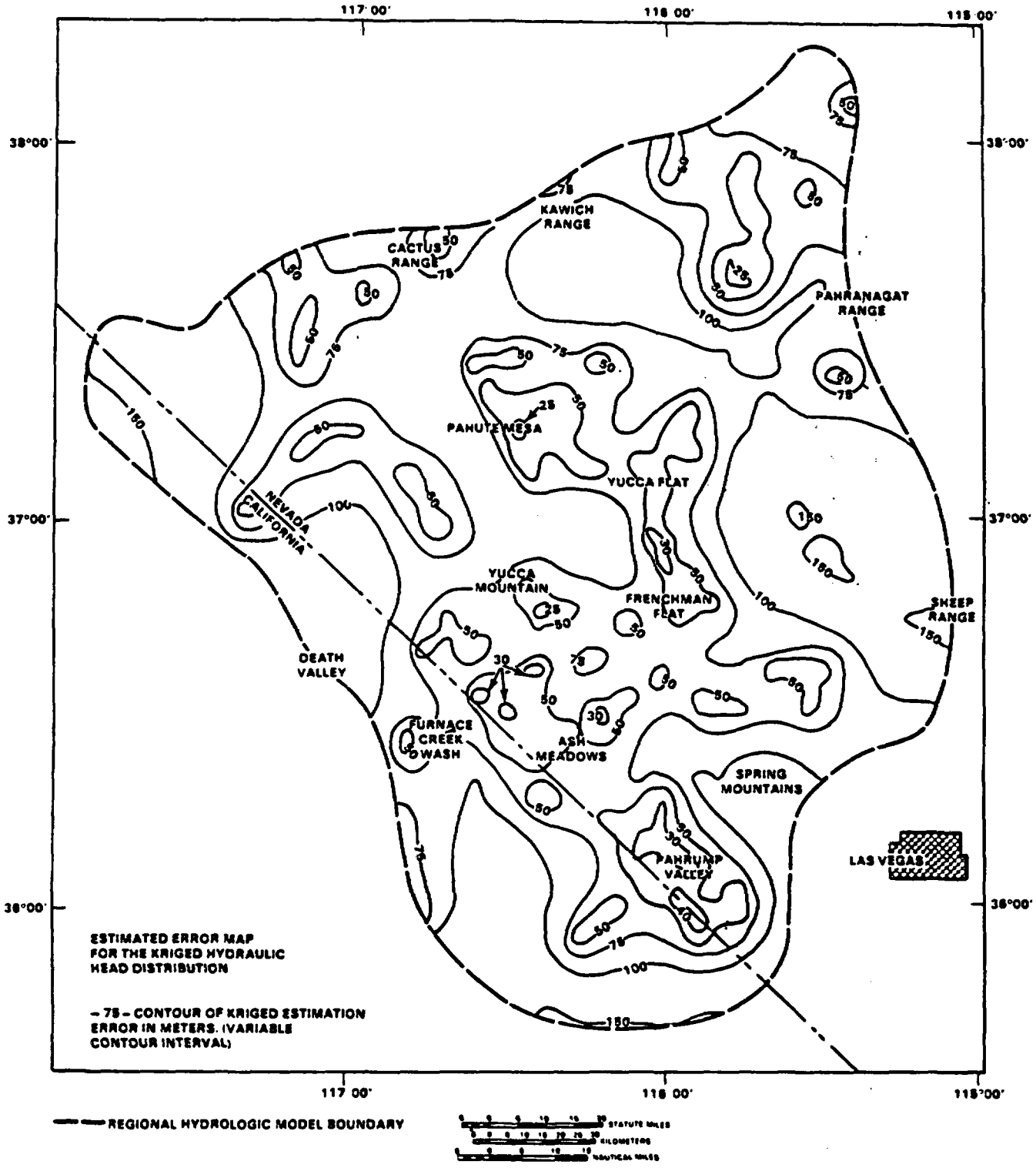

FIGURE 8. Map of Kriging Error or Estimation Error for the Regional Model (contours in meters of error)

Net recharge to the ground water depends on many climatic and hydrologic parameters. Some of the more important parameters considered in a detailed recharge calculation are as follows:

- Precipitation--Precipitation directly supplies water to the hydrologic system. Both the total amount and rate of water reaching the ground surface influence the amount of recharge. When the rate of precipitation exceeds the capacity for infiltration of a soil, runoff occurs. An amount of precipitation in excess of the capacity for water storage in a soil results in recharge to the ground-water system.
- Soil properties--Soil properties of infiltration capacity, water-holding capacity, and soil depth influence recharge. Properties of the soil control the amount of water that moves through the soil to the aquifer or remains in storage and available for use by vegetation.
- Climatic parameters--Climatic parameters other than precipitation influence recharge. A combination of air temperature, relative humidity, net solar radiation, and wind velocity provide atmospheric demand for removal of water from the hydrologic system by vaporization. This atmospheric demand is termed potential evapotranspiration (PET).
- Characteristics of vegetation--The extent of canopy cover and rooting depth of vegetation also influences recharge. Direct loss of intercepted water and transpiration makes vegetation an efficient extractor of water.
- Topography--Topography of the modeled region is important because precipitation runoff and other climatic parameters can be correlated with elevation.

Recharge was calculated by a water balance over the root zone of the vegetation, where

$$\text{Recharge} = \text{Precipitation} - \text{Runoff} - \text{Actual Evapotranspiration} \pm \Delta\ \text{Soil Storage}$$

Of the terms involved in calculating recharge, estimates of evapotranspiration pose the most difficult problem. We used the concept of PET to define the amount of water that would be removed from the land surface by

by evaporation and transpiration processes if sufficient water were available in the soil to meet the demand. Actual evapotranspiration (AET), on the other hand, is that portion of PET that is actually transpired under a limited supply of soil moisture. Actual evapotranspiration depends on the unsaturated moisture storage properties of the soil and vegetative factors such as plant type and stage of growth. The empirical Blaney-Criddle relationship (Blaney and Criddle 1950) was used to estimate PET. Then PET was converted to AET by the Thornthwaite and Mather (1955) linear decrease soil moisture relationship.

The best estimate of recharge is 1.33×10^5 acre-feet per year. This estimate is based on recharge from precipitation falling within the confines of the hydrologic model and does not include flux entering as underflow from the mountains to the north and east of the model boundaries (see section on Water Balance Calculations). The distribution of recharge is presented in Figure 9. Based on a sensitivity analysis, estimates of recharge may range from 5.3×10^4 to 2.1×10^5 acre-feet per year. A detailed discussion of the recharge calculation and a sensitivity analysis of recharge parameters is presented in Appendix A.

DISCHARGE

Discharge from the regional model occurs naturally through evapotranspiration and springs, and artifically through pumping. Net discharge was considered on the basis of geographic locations. Table B.2 in Appendix B provides a summary of tables and plates from the reference sources listed in Table B.1 that were consulted while estimating the net discharge (stress minus recycled water) for each location in the study area.

Discharge areas (Fig. 10) were digitized from maps and plates listed in Table B.2, and then overlayed on a node map so that an appropriate net discharge value could be assigned to a node or distributed over several nodes. Table B.3 lists the node coordinates and net discharges assigned to each.

Each discharge type, the percentage each type contributes to the total discharge, and the uncertainty in each discharge estimate is presented in

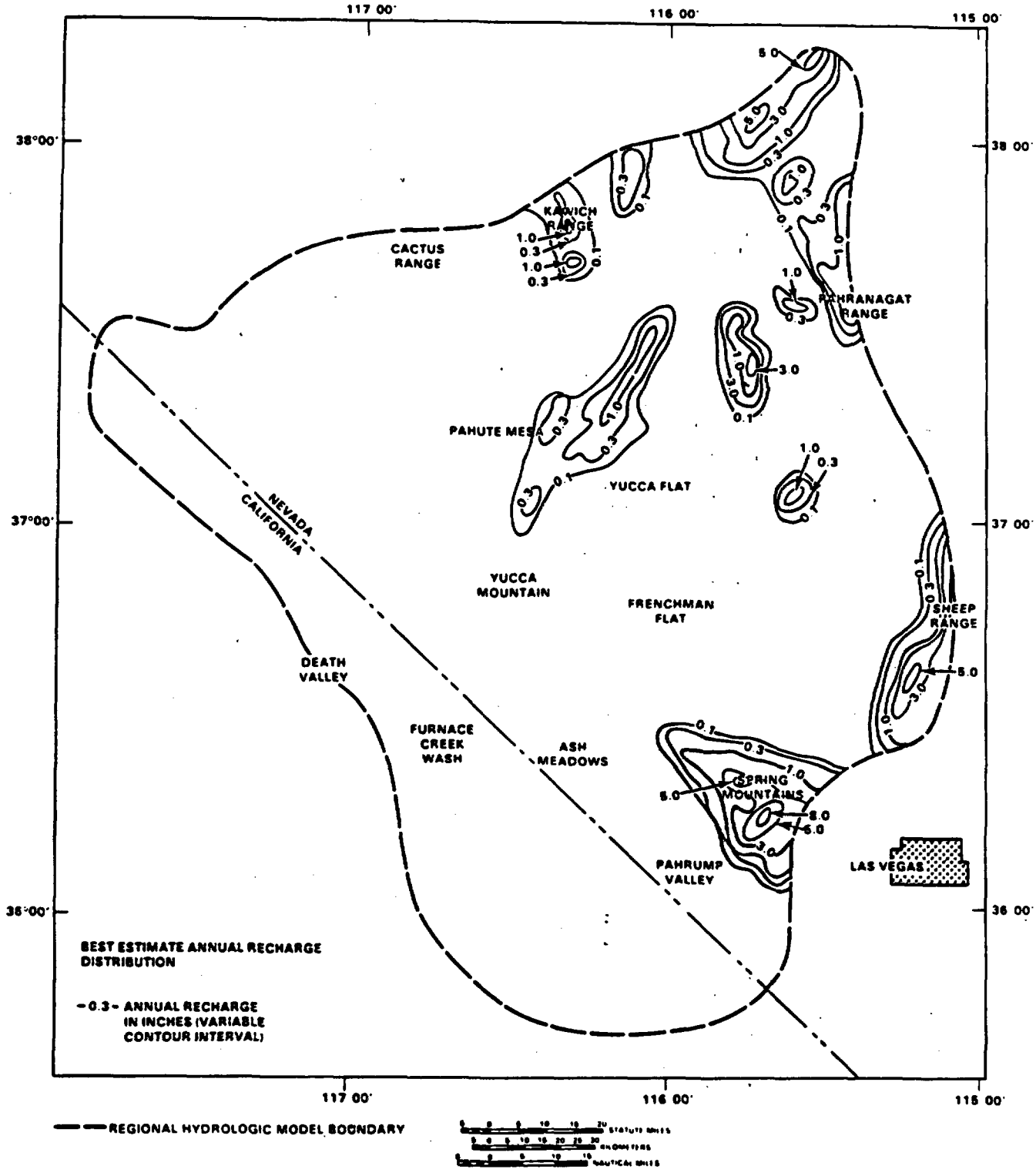

FIGURE 9. Best Estimate Annual Recharge Distribution for the Regional Model

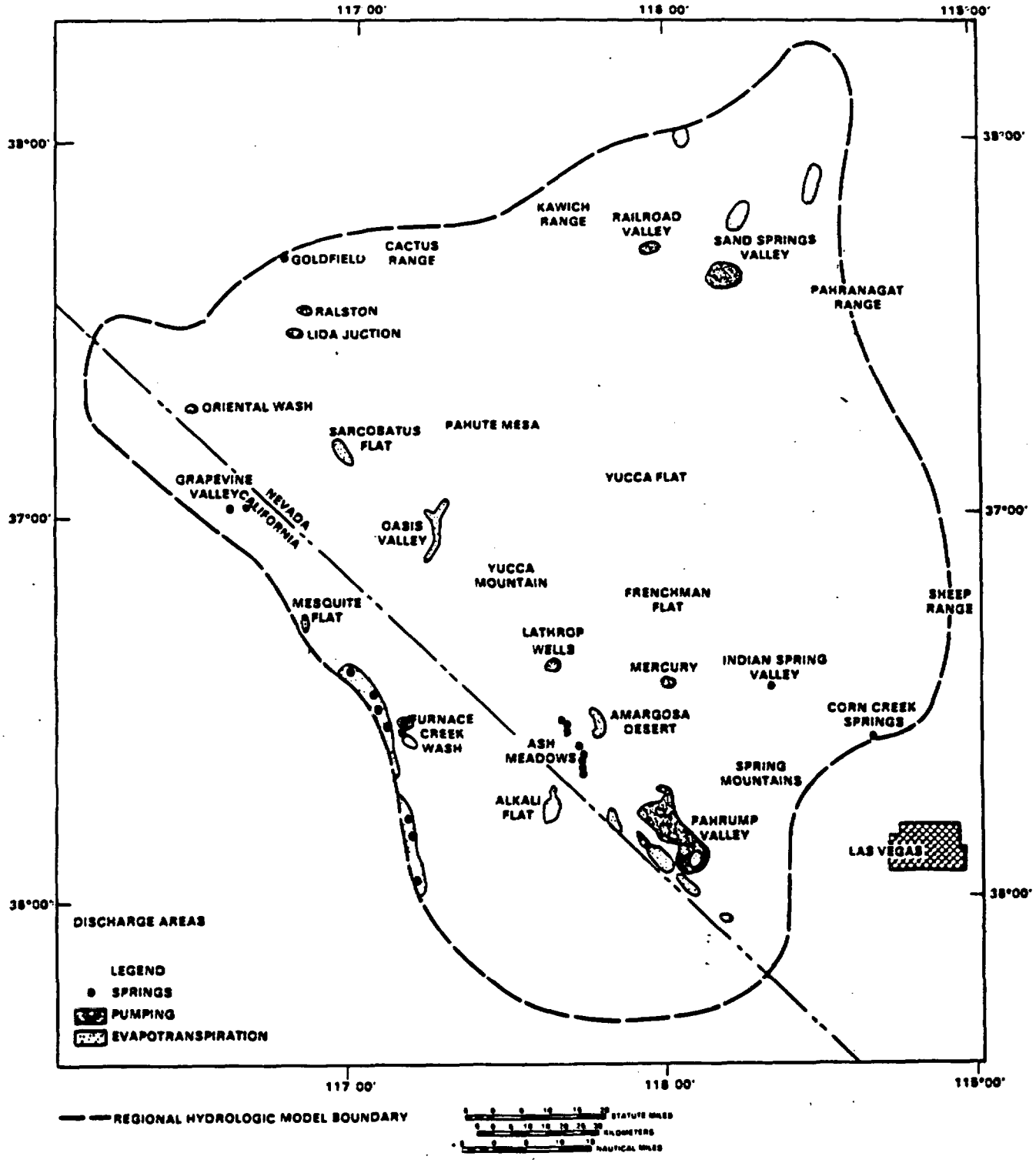

FIGURE 10. Discharge Areas of the Regional Model

Table 2. Evapotranspiration in discharging areas has the highest degree of uncertainty because a mean consumptive use rate for several species of phreatophytes is assumed rather than considering a consumptive use rate dependent on the areal distribution of each species. The evapotranspiration value listed in Table 2 does not include evaporation occurring in Death Valley.

TABLE 2. Summary of Net Discharges with Uncertainty Bounds for the Regional Model

Discharge Type	Net Discharge Discharge (acre-ft/yr)	Percent of Total Discharge	Uncertainty Bounds (%)
Springs	3.06×10^4	32	±25
Pumping	4.77×10^4	51	±20
Evapotranspiration	1.59×10^4	17	±35
Total	9.42×10^4	100	

TRANSMISSIVITY

Initial estimates of transmissivity for the regional model were taken from the USGS regional hydrologic model (Waddell 1982). For those geographic areas of the PNL regional model that were not included in the USGS regional model, initial zones of transmissivity were estimated by creating less transmissive zones where uplifting had occurred in mountainous areas. Thus, Spring Mountain, Sheep, Kawich, Reveille, Quinn Canyons, and Amargosa Ranges were initially assigned transmissivities one to two orders of magnitude lower than their valley counterparts. Because uncertainty in transmissivity is greater than the uncertainty in the stress and recharge calculation, the former parameter was adjusted during the numerous model calibration runs. The final calibrated transmissivity distribution is presented in Figure 11.

MODEL CALIBRATION

Model calibration involved adjusting the transmissivities within reasonable limits in order to minimize the difference between the hydraulic heads simulated by the model and hydraulic heads measured at well locations.

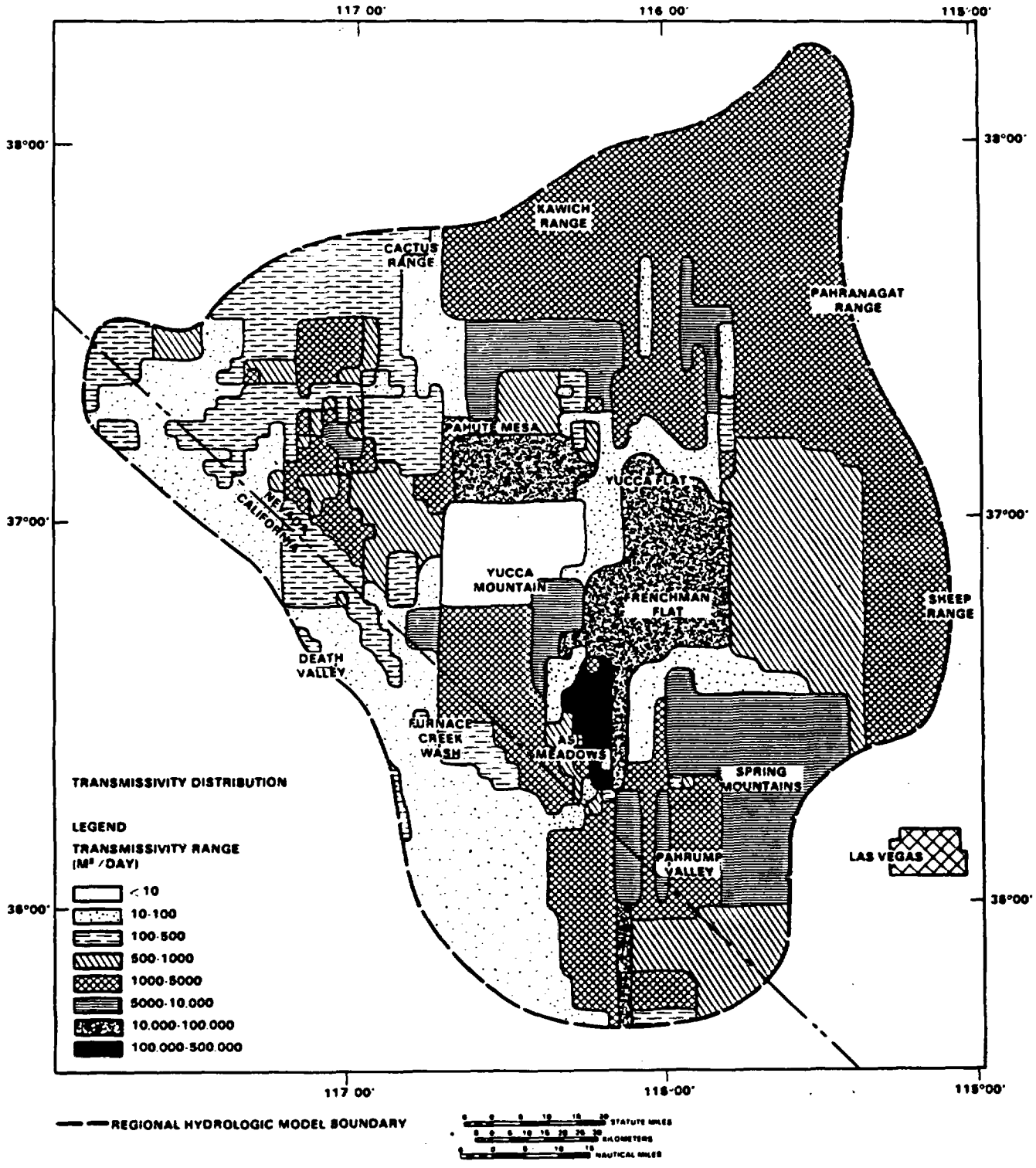

FIGURE 11. Transmissivity Distribution for the Calibrated Regional Model

The basis for determining when the residual error (difference between predicted and measured head) is sufficiently minimized was approached in the following manner. First, hand contouring by the USGS of the hydraulic head distribution shown in Figure 6 involved a certain amount of subjective interpretation. As previously discussed, the accuracy of this interpretation can be measured by the average and root-mean-squared error difference between the predicted heads and measured heads. If the differences between heads predicted by the model and measured heads are equal to or better than the average and root-mean-squared error of the hand-contoured head distribution, then the model is considered calibrated within the accuracy of the data. A statistical comparison of the hydraulic heads interpreted by the USGS and the hydraulic heads predicted by the model versus observed heads at well locations is summarized in Table 3.

TABLE 3. Comparison of Calibration Statistics for the Regional Model Under Steady-State Confined Conditions (units in meters)

Calibration Statistic	USGS-Interpreted Hydraulic Heads Versus Well Observations	Model-Predicted Hydraulic Heads Versus Well Observations
Average Difference	23.7	47.3
Root-Mean-Squared Difference	34.3	58.8
Maximum Positive Difference	177.3	207.8
Maximum Negative Difference	-117.0	-96.2

The ranges of residual error for the USGS-interpreted head distribution and the head distribution predicted by the model are summarized in Table 4.

The kriging error was also considered in determining the level of model calibration. When the kriging error is small (see Fig. 8), there are more hydraulic head data, and thus, more certainty in the hydraulic head distribution. The model calibration concentrated on minimizing the error residuals in the areas of the hydrologic model where the kriging error is small, especially in the localized vicinity of Yucca Mountain, which is the primary focus of this study.

TABLE 4. Residual Error Distribution Summary for USGS-Interpreted Hydraulic Heads and Model-Predicted Hydraulic Heads Versus Well Observations

Residual Error Range (m)	Wells with Residual Errors			Wells with Negative Residual Errors			Wells with Positive Residual Errors		
	Absolute Number	%	Cumulative %	Absolute Number	%	Cumulative %	Absolute Number	%	Cumulative %
USGS-INTERPRETED HYDRAULIC HEADS VERSUS WELL OBSERVATIONS									
0. - 50.	140	85.4	85.4	35	21.3	21.3	105	64.0	64.0
50. - 100.	21	12.8	98.2	4	2.4	23.8	17	10.4	74.4
100. - 150.	2	1.2	99.4	1	0.6	24.4	1	0.6	75.0
150. - 200.	1	0.6	100.0	0	0.0	24.4	1	0.6	75.6
200. - 250.	0	0.0	100.0	0	0.0	24.4	0	0.0	75.6
Totals	164			40			124		

Residual Error Range (m)	Wells with Residual Errors			Wells with Negative Residual Errors			Wells with Positive Residual Errors		
	Absolute Number	%	Cumulative %	Absolute Number	%	Cumulative %	Absolute Number	%	Cumulative %
MODEL-PREDICTED HYDRAULIC HEADS VERSUS WELL OBSERVATIONS									
0. - 50.	91	55.5	55.5	13	7.9	7.9	78	47.6	47.6
50. - 100.	58	35.4	90.9	23	14.0	22.0	35	21.3	68.9
100. - 150.	14	8.5	99.4	0	0.0	22.0	14	8.5	77.4
150. - 200.	0	0.0	99.4	0	0.0	22.0	0	0.0	77.4
200. - 250.	1	0.6	100.0	0	0.0	22.0	1	0.6	78.0
Totals	164			36			128		

The best steady-state simulation for calibration under confined conditions is shown in Figure 12. The shape of the predicted hydraulic head distribution generally agrees with the kriged and USGS-interpreted hydraulic head distributions (compare Fig. 12 with Fig. 6 and 7). The residual errors in the vicinity of Yucca Mountain range between 12 and 24 meters. Higher residual errors occur upgradient in the Pahute Mesa area. Given the assumption of modeling in two dimensions, the vertical movement of ground water in Pahute Mesa may preclude calibration of the model in this local area (Waddell 1982). The residual errors in Pahrump Valley range between 30 and 70 meters. Effort was not expended to significantly reduce these errors because the westward movement of ground water from the Spring Mountains into Pahrump Valley is independent of the hydrologic system affecting Yucca Mountain.

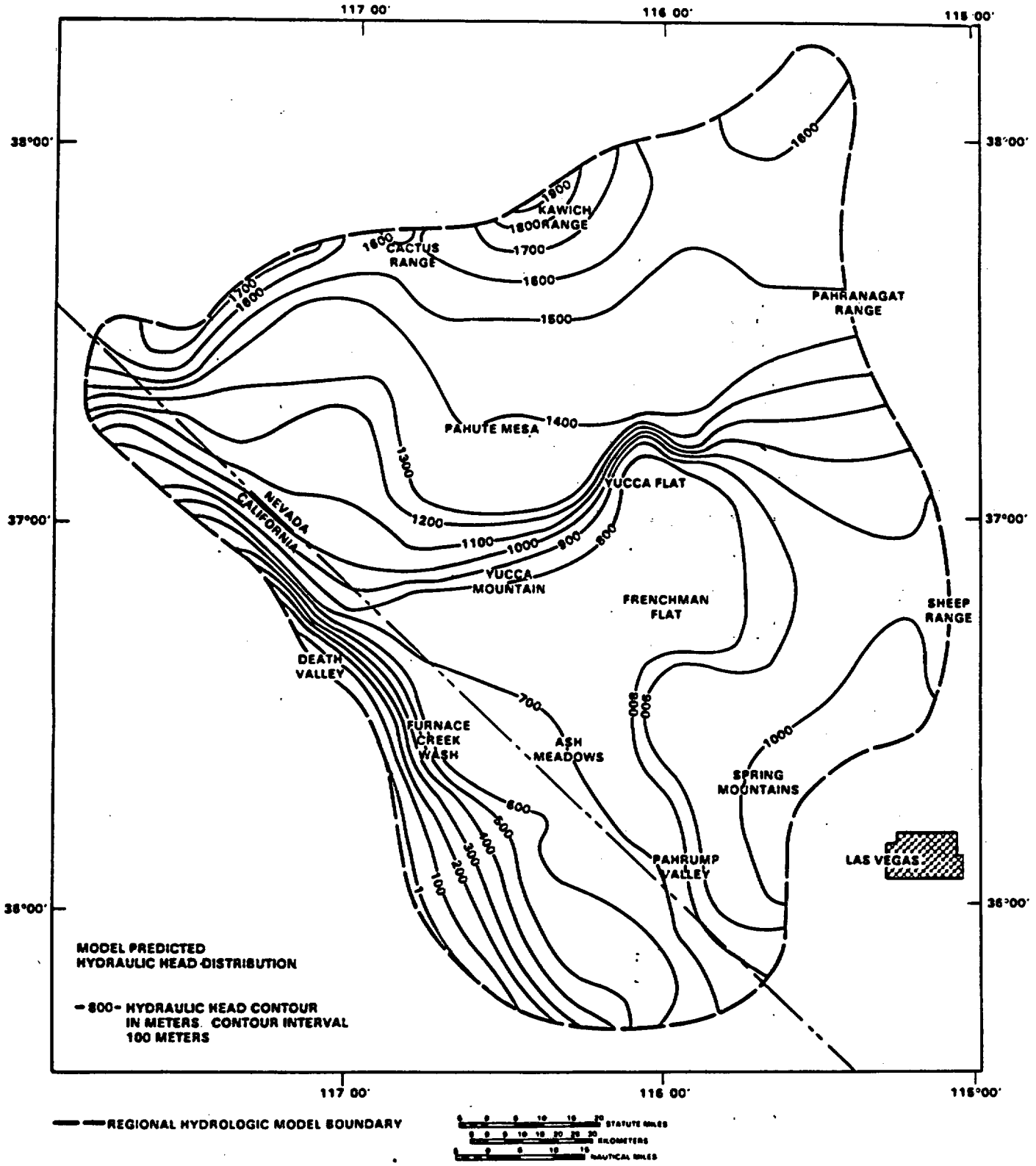

FIGURE 12. Model-Predicted Hydraulic Heads for Steady-State Confined Conditions (hydraulic heads in meters above MSL)

WATER BALANCE CALCULATIONS

During the data collection process, an effort was made to review the literature so that the recharge and discharge values estimated for the hydrologic model could be compared to reported estimates. The water balance estimate for about 90% of the catchment basins in our study area is 131,000 acre feet per year. This estimate was calculated by the Walker-Eakin method and reported by the State of Nevada, Department of Conservation and Natural Resources in the Water Resources Reconnaissance Series Reports No. 7, 18, 45, 54. The recharge estimate, 133,000 acre feet per year, predicted for the regional hydrologic model is in good agreement with the estimate calculated by the Walker-Eakin method. The total flow into the hydrologic model, 227,000 acre feet per year, consists of recharge from precipitation and underflow into the model from the north and east. Discharge from the model is the total discharge from springs, pumping, and evapotranspiration (94,200 acre feet per year); plus discharge from the constant head boundary nodes of Death Valley and the southern boundary. The total model discharge is 226,000 acre feet per year. A summary of the water balance for the hydrologic model is presented in Table 5.

TABLE 5. Water Balance Summary for the Regional Model

Flux into the Model	Estimate of Prediction (acre-ft/yr)
PNL's estimate of recharge from precipitation (see Appendix A)	1.33×10^5 [a]
Predicted underflow entering the model along the north and east boundaries (this includes flow entering along Spring Mountain)	9.47×10^4
TOTAL	2.27×10^5
Flux out of the Model	
Estimate of net discharge from pumping, springs, and evapotranspirtation	9.42×10^4
Predicted underflow leaving the model from Death Valley, and along the southern boundary	1.32×10^5
TOTAL	2.26×10^5

(a) The recharge estimate predicted by Walker-Eakin method is 1.31×10^5 acre feet per year. (Estimate accounts for approximately 90% of the catchment basins in the modeled region.)

SUMMARY AND RECOMMENDATIONS

The model-predicted hydraulic head distribution presented in Figure 12 indicates that PNL has a working regional model of the Nevada Test Site. Water balances within the modeled region indicate that calculated estimates of recharge and discharge are in good agreement with published values.

The recharge calculation presented in this report is the first published source documenting a detailed estimate of recharge for this study area. The sensitivity analysis for calculation of recharge provides insight into the plausible uncertainty of the estimate. However, it should be emphasized that no matter how accurate the estimate of recharge, a significant amount of flux enters the study area by underflow from recharge to the carbonate aquifer in mountainous areas to the north and east of the model.

There are obvious refinements to the model that can be readily made at this time. Accuracy of the model may be improved by the following:

- calibrating the model under unconfined conditions
- incorporating the latest USGS measurements of hydraulic head into the hydrologic model
- analyzing well logs of the 240 wells considered in this study and incorporating only the reliable hydraulic head measurements and aquifer tests in the model.

Other refinements that are highly recommended but would require greater effort and expenditures are listed below:

- The model should be calibrated with a statistical parameter estimation technique that minimizes the difference between predicted and observed hydraulic heads and estimates the uncertainty in the predicted hydraulic heads and calibrated transmissivities.
- A three-dimensional hydrologic model should be constructed consisting of two layers: the top layer representing the alluvial and volcanic aquifers, and the bottom layer representing the carbonate aquifer. Such a three-dimensional model would more accurately simulate the physical system, particularly, where vertical flow occurs. Analysis of well logs and keying the hydraulic heads and aquifer tests to specific hydrostratigraphic units would allow construction of a three-dimensional model.

REFERENCES

Blankennagel, R. K. and J. E. Weir. 1973. Geohydrology of the Eastern Part of Pahute Mesa, Nevada Test Site, Nye County, Nevada. U.S. Geol. Surv. Prof. Paper 712-B, p. B.1-B.35.

Blaney, H. F. and W. D. Criddle. 1950. "Determining Water Requirements in Irrigated Areas from Climatological and Irrigation Data." USDA (SCS). TP-6.

Clebsch, Jr., A. and F. B. Barker. 1960. Analyses of Ground Water from Rainier Mesa, Nevada Test Site, Nye County, Nevada. U.S. Geol. Surv. Open-File Report TEI-763.

Devary, J. L. and W. A. Rice. 1983. Geostatistical Software User's Manual for the Geosciences Research and Engineering VAX Computer System. PNL-4882 Pacific Northwest Laboratory, Richland, Washington.

Eakin, T. E. 1966. "A Regional Interbasin Groundwater System in the White River Area, Southeastern Nevada." Water Resources Research 2(2): 251-271.

Eakin, T. E., T. E. Maxey, G. B. Robinson, J. C. Fredericks and O. G. Loeltz. 1951. Contributions to the Hydrology of Eastern Nevada. Nevada State Engineers, Water Resources Bulletin, No. 12, p. 171.

Eakin, T. E. and D. O. Moore. 1964. Uniformity of Discharge of Muddy River Springs Southeastern Nevada and Relation to Interbasin Movement of Ground Water. U.S. Geol. Surv. Prof. Paper 501-D, p. D171-D176.

Eakin, T. E. and I. J. Winograd. 1965. "Interbasin Movement of Ground Water in Southcentral Nevada--Some Implications." In Abstracts for 1964: Geol. Soc. America Spec. Paper 82, p. 52.

Freeze, R. A. and J. A. Cherry. 1979. Groundwater. Prentice-Hall Inc., Edgewood Cliffs, New Jersey.

Freeze, R. A. and P. A. Witherspoon. 1966. "Theoretical Analysis of Regional Ground-Water Flow; (1) Analytical and Numerical Solutions to the Mathematical Model." Water Resources Research 2(4):641-656.

Freeze, R. A. and P. A. Witherspoon. 1967. "Theoretical Analysis of Regional Ground-Water Flow; (2) Effect of Water-Table Configuration and Subsurface Permeability Variation." Water Resources Research 3(2):623-634.

Grove, D. B., M. Rubin, B. B. Hanshaw and W. A. Beetem. 1969. Carbon-14 Dates of Ground Water from a Paleozoic Carbonate Aquifer, Southcentral Nevada. U.S. Geol. Survey Prof. Paper 650-C, p. C215-C218.

Hunt, C. B. and T. W. Robinson. 1960. Possible Interbasin Circulation of Ground Water in the Southern Part of the Great Basin. U.S. Geol. Survey Prof. Paper 400-B, p. B273-B274.

Hunt, C. B., T. W. Robinson, W. A. Bowles and A. L. Washburn. 1966. Hydrologic Basin, Death Valley, California. U.S. Geol. Surv. Prof. Paper 494-B, 138 p.

Loeltz, O. J. 1960. "Source of Water Issuing from Springs in Ash Meadow Valley, Nye County, Nevada" (abstract). Geol. Soc. America Bull. 71:1917-1918.

Malmberg, G. T. and T. E. Eakin. 1962. Ground-Water Appraisal of Sarcobatus Flat and Oasis Valley, Nye and Esmeralda Counties, Nevada. Nevada Dept. Converv. and Nat. Resources, Reconn. Ser. Report 10, 39 p.

Maxey, G. B. 1968. "Hydrogeology of Desert Basins." Ground Water. 6(5):10-22.

Maxey, G. B. and C. H. Jameson. 1948. Geology and Water Resources of Las Vegas, Pahrump, and Indian Springs Valleys, Clark and Nye Counties, Nevada. Nevada State Engineer Water Resources Bulletin No. 5.

Maxey, G. B. and M. D. Mifflin. 1966. "Occurrence and Movement of Ground Water in Carbonate Rocks of Nevada." Natl. Speleol. Soc. Bull. 28(3):141-157.

Miller, G. A. 1977. Appraisal of the Water Resources of Death Valley, California-Nevada. U.S. Geol. Surv. Open-File Report 77-728, 67 p.

Moore, G. E. 1961. Records of Wells, Test Holes, and Springs in the Nevada Test Site and Surrounding Area. U.S. Geol. Surv. Open-File Report TEI-781, 22 p.

Oberlander, P. L. 1979. Development of a Quasi Three-Dimensional Groundwater Model for a Portion of the Nevada Test Site. NVO-1253-14, Water Resources Center, Desert Research Institute, University of Nevada, Reno, Nevada.

Pistrang, M. A. and F. Kunkel. 1964. A Brief Geologic and Hydrologic Reconnaissance of the Furnace Creek Wash Area, Death Valley National Monument, California. U.S. Geol. Surv. Water-Supply Paper 1779-Y, 35 p.

Reisenauer, A. E. 1980. Variable Thickness Transient Groundwater Hydrologic Model, (3 volumes). PNL-3160, Pacific Northwest Laboratory, Richland, Washington.

Sass, G. H. and A. H. Lachenbruch. 1982. Preliminary Interpretation of Thermal Data from the Nevada Test Site. U.S. Geol. Surv. Open-File Report (in review).

Schoff, S. L. and Moore, G. E. 1964. Chemistry and Movement of Ground Water, Nevada Test Site. U.S. Geol. Surv. Open File Report TEI-838, 75 p.

Thornthwaite, L. W. and G. R. Mather. 1955. "The Water Balance." Laboratory of Climatology, Publication No. 8, Centerton, New Jersey.

Waddell, R. K. 1982. Two-Dimensional, Steady-State Model of Ground-Water Flow, Nevada Test Site and Vicinity, Nevada-California. U.S. Geol. Surv. Water Resources Investigations 81-4085, Denver, Colorado.

Walker, G. E. and T. E. Eakin. 1963. Geology and Ground Water of Amargosa Desert, Nevada-California. Nevada Dept. Conserv. and Nat. Resources, Reconn. Ser. Report 14, 45 p.

Winograd, I. J. 1962. Interbasin Movement of Ground Water at the Nevada Test Site, Nevada. U.S. Geol. Survey Prof. Paper 450-C, p. C108-C111.

Winograd, I. J. 1971. Origin of Major Springs in the Amargosa Desert of Nevada and Death Valley California. Ph.D Dissertation, University of Arizona, Tucson, Arizona.

Winograd, I. J. 1981. "Radioactive Waste Disposal in Thick Unsaturated Zones." Science. 212(4502):1457-1464.

Winograd, I. J. and G. C. Doty. 1980. Paleohydrology of the Southern Great Basin, with Special Reference to Water Table Fluctuations Beneath the Nevada Test Site During the Late (?) Pleistocene. U.S. Geol. Surv. Open-File Report 80-569, 97 p.

Winograd, I. J. and I. Friedman. 1972. "Deuterium as a Tracer of Regional Ground-Water Flow, Southern Great Basin, Nevada and California." Geol. Soc. America Bull. 83(12):3691-3708.

Winograd, I. J. and W. Thordarson. 1975. Hydrogeologic and Hydrochemical Framework South-Central Great Basin, Nevada-California, with Special Reference to the Nevada Test Site. U.S. Geol. Surv. Prof. Paper 712-C, 126 p.

APPENDIX A

DETAILED RECHARGE CALCULATION

A detailed recharge calculation was considered essential for the regional hydrologic simulation of the Nevada Test Site (NTS) and vicinity because the transmissive properties of the major water-bearing units are not well defined. An estimate of the amount of water transmitted through the alluvial, volcanic, and carbonate aquifer systems is required to bound the transmissivity values. Additionally, such a recharge calculation has not been performed for this study area.

The objective of this appendix is to present a detailed explanation of the recharge calculation. The calculation performed for this study used distributed meteorologic, plant, and soil moisture data. While precipitation within the model area is a major source of recharge to the ground-water system, the reader should bear in mind that the north and east boundaries of the modeled region are held to allow flux or underflow into the model from recharge occurring in the mountains that extend to the north and east of the model boundary. This flux also contributes to the total flow in the hydrologic model.

Recharge for the model was calculated by a water balance over the root zone of vegetation. The water balance implies that incoming water must equal outgoing water plus changes in soil water storage:

$$\text{Recharge} = \text{Precipitation} - \text{Runoff} - \text{Actual Evapotranspiration} \pm \Delta\ \text{Soil Storage}$$

The following sections will discuss the data sources and methodology used to determine the areal distributions of the recharge parameters in the equation above. Also presented is a sensitivity analysis that brackets the recharge estimate by varying the most uncertain parameters of the equation for recharge.

PRECIPITATION

Precipitation in Nevada south of 38-1/2° latitude can be divided into two zones (Quiring 1965). These zones are the result of major topographical and meteorological features that influence precipitation. During the winter,

the moisture approaches the NTS from the Pacific Ocean. Moisture is carried eastward by prevailing westerly winds as shown in Figure A.1. The Sierra Nevada Range imposes an extensive barrier that depletes the moisture and results in a rain shadow or deficit of precipitation east of the range. In the summer, moisture approaches the NTS from the southeast and south and is brought into Nevada by frequent winds from the gulf area that curve north and then east (see Fig. A.1).

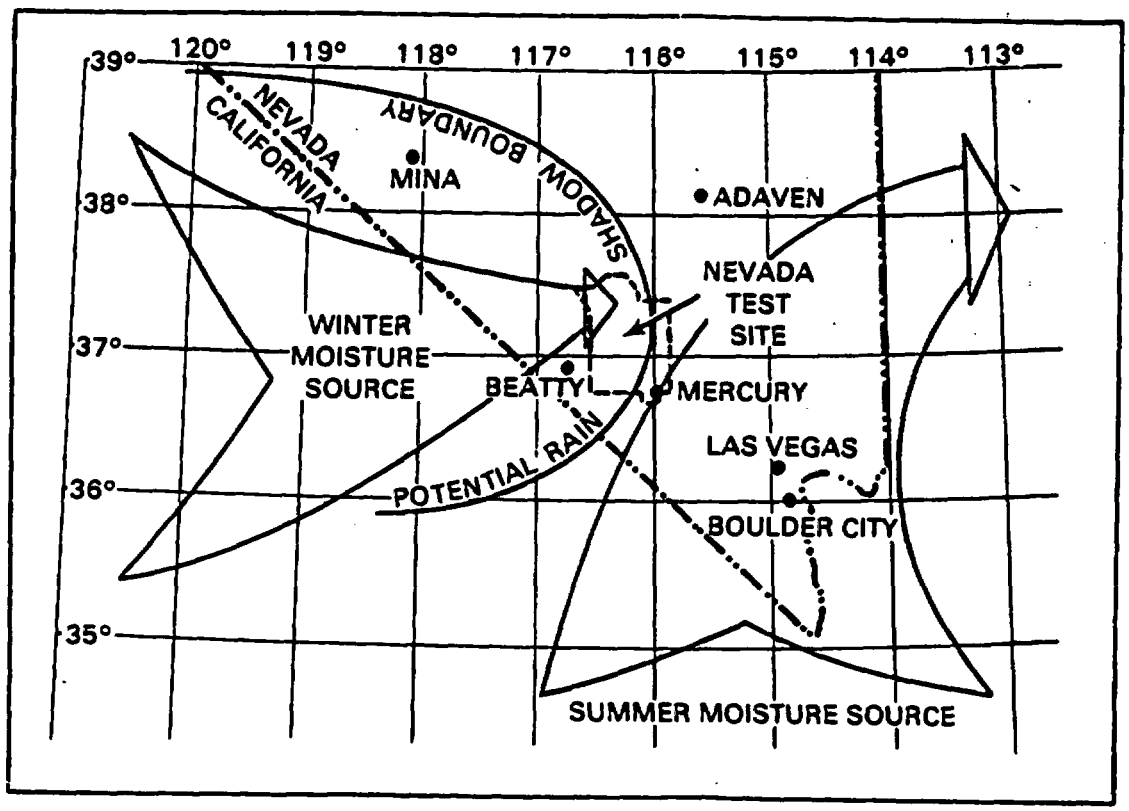

FIGURE A.1. Summer and Winter Moisture for the Southern Nevada Area (from French 1983)

The net effect of these two phenomena is a zone of relative precipitation excess in the southeastern portion of the state and a deficit zone in the southwestern portion of the state. Two researchers, Quiring (1965) and French (1983) have documented this pattern by regressing the logarithm of normalized annual precipitation data from weather stations in southern Nevada versus elevation. While the fit of the linear regression is not good when all stations are considered, the grouping of stations above and below the regression line

suggests that three regression lines based on an areal separation of stations into deficit, transition, and excess zones are required for a better fit. The three regression equations derived by considering only excess stations, only deficit stations, and both (Quiring 1965) are:

$$\text{(Excess)} \quad \log(\bar{p}) = 0.331 + (6.7 \times 10^{-5})\ E$$
$$\text{(Deficit)} \quad \log(\bar{p}) = 0.397 + (8.9 \times 10^{-5})\ E$$
$$\text{(Transition)} \quad \log(\bar{p}) = 0.316 + (9.4 \times 10^{-5})\ E$$

where $\bar{p}$ is annual average precipitation in inches per year and E is station elevation in feet. The regression equations with the boundaries of the relative moisture zones as they apply to our model region are shown in Figure A.2. The resulting areal distribution of annual precipitation, given the above regression equations and the topographic elevation, is shown in Figure A.3.

For the purposes of this study, recharge calculations were made on a monthly basis. Annual precipitation was partitioned into monthly values using the normalized curve shown in Figure A.4. This curve was determined by computing the mean fraction of annual precipitation occurring for each month for the 35 weather stations listed in Table A.1 (NOAA 1981a,b).

Topography

Topographic data were acquired from the digital terrain tapes, obtained from the National Cartographic Information Center, U.S. Geological Survey (USGS), U.S. Department of Interior. Figure A.5 shows the topographic data interpolated to the 12,500-foot grid system used in the hydrologic model. The topographic distribution was used in calculating both the precipitation and potential evapotranspiration (PET) distributions since a correlation exists between these two parameters and elevation. The topographic distribution was also used to calculate the maps of soil and vegetation that served as input to the calculation of actual evapotranspiration (AET).

ACTUAL EVAPOTRANSPIRATION

Actual evapotranspiration is the actual rate of evapotranspiration for a given climatic condition, soil moisture status, and plant species. Computing AET is not a straightforward procedure. Therefore, a discussion of each

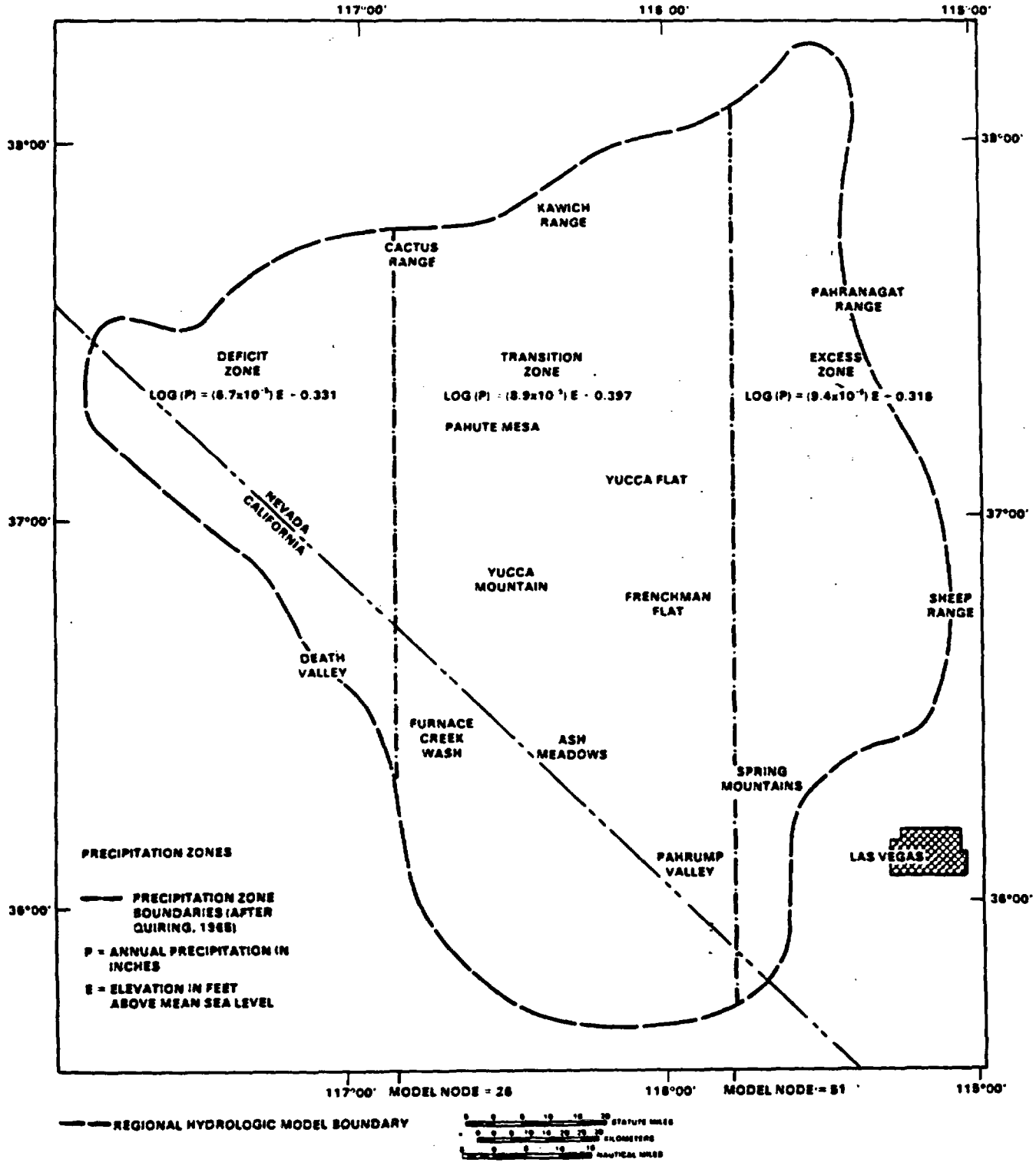

FIGURE A.2. Precipitation Zones and Regression Functions used to Calculate the Annual Precipitation Distribution

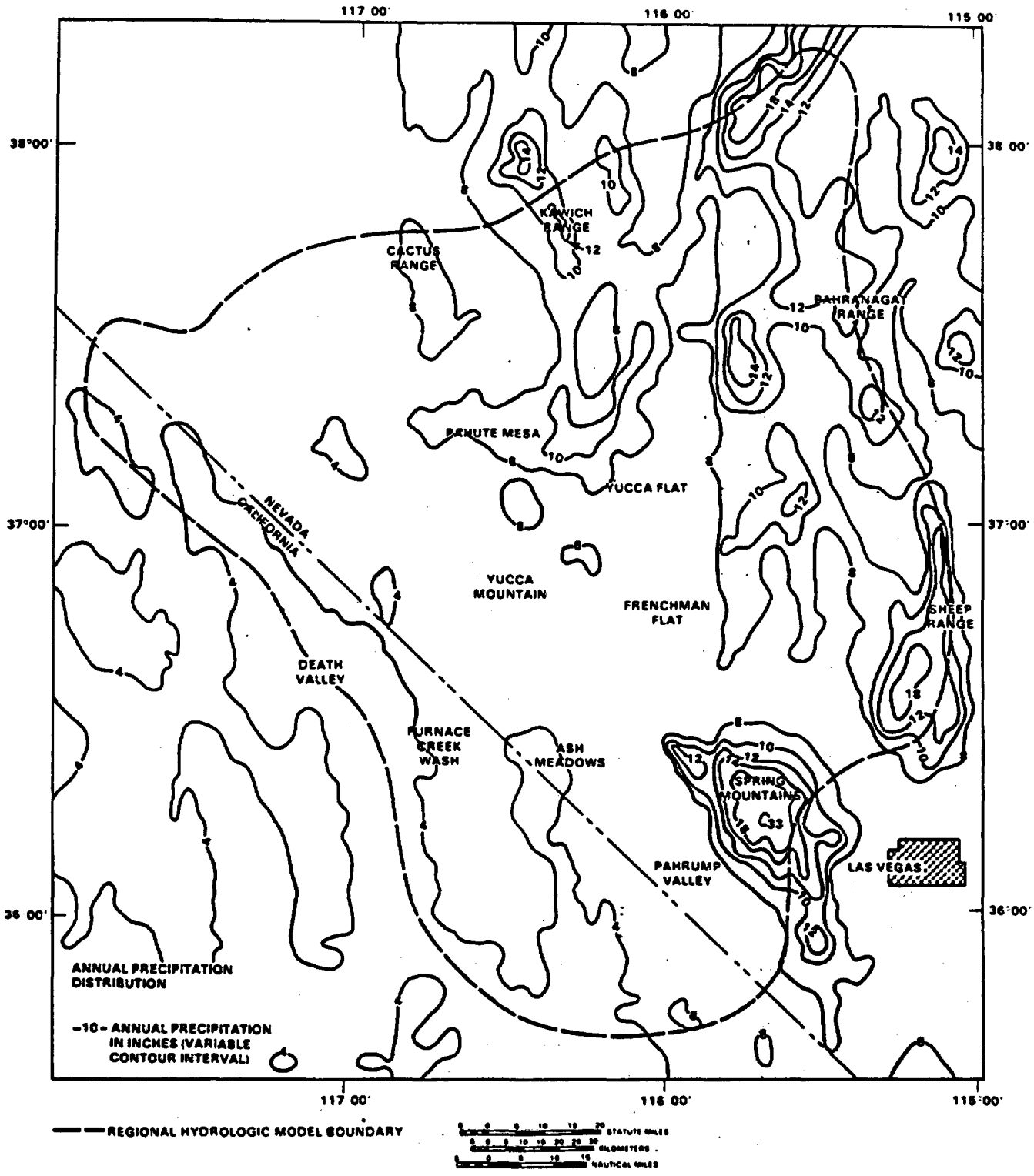

FIGURE A.3. Annual Precipitation Distribution

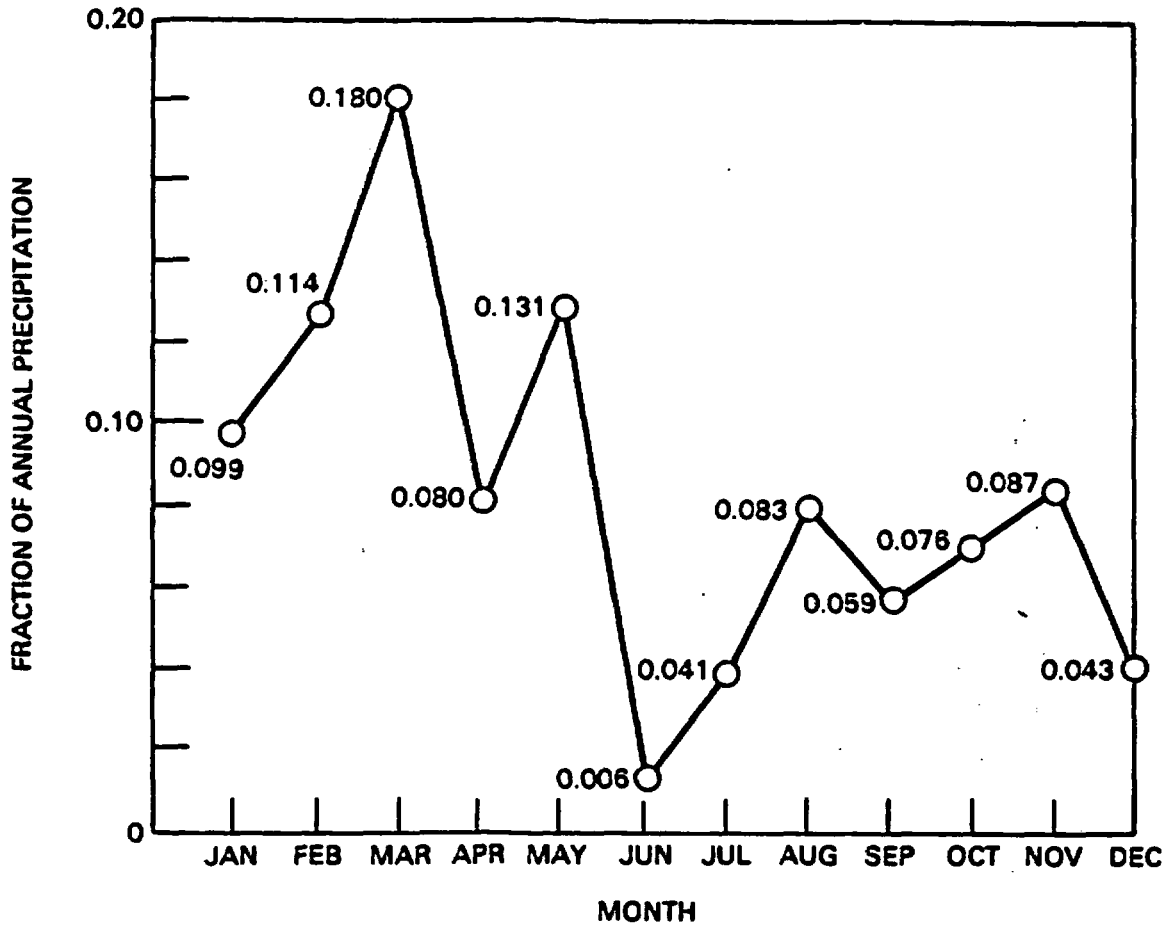

FIGURE A.4. Monthly Fraction of Annual Precipitation used to Calculate Monthly Precipitation Distributions

variable contributing to the calculation of AET is provided in the following sections.

Potential Evapotranspiration

Actual evapotranspiration is always equal to or smaller than PET, which is defined as the rate of evapotranspiration of a short, green crop unlimited by deficiencies of water supply (Dunne and Leopold 1978). Numerous methods are available for calculating PET. The Blaney and Criddle method (Blaney and Criddle 1950) used in this study is somewhat limited in accuracy because it depends on a single climatic variable, temperature, and the use of an empirical crop coefficient that is influenced by climatic conditions. However, use of the Blaney and Criddle formula (Blaney and Criddle 1950) is justified because 1) no Class A weather stations are within the model region to provide the

TABLE A.1. Meteorological Stations Used to Calculate the Precipitation and Potential Evapotransportation Distributions

No.	Weather Station[a]	Latitude(N) deg.	Latitude(N) min	Longitude(W) deg.	Longitude(W) min	Elev. (ft)	Period of Record (yr) Precip.	Period of Record (yr) Temp.
1	Adaven	38	07	115	35	6250	66	68
2	Amargosa Farms-Garey	36	34	116	28	2450	10	10
3	Beatty 8 N	37	00	116	43	3550	10	10
4	Desert Natl Wldlf Rng	36	26	115	22	2920	36	40
5	Dyer 4SE	37	37	118	01	4975	27	29
6	Goldfield	37	42	117	14	5690	56	58
7	Key Pittman WMA	37	37	115	13	3950	18	18
8	Los Vegas WSO AP	36	05	115	10	2162	45	45
9	Pahranagat W L Refuge	37	16	115	07	3400	18	18
10	Pahrump	36	12	115	59	2670	24	25
11	Red Rock Canyon St Pk	36	05	115	27	3780	05	05
12	Silverpeak	37	40	117	35	4263	15	15
13	Sunrise Manr Las Vegas	36	12	115	05	1820	30	30
14	Tempiute 4 NW	37	41	115	43	4890	10	10
15	Tonopah AP	38	04	117	05	5426	27	27
16	Death Valley	36	28	116	52	-194	65	69
17	Deep Springs College	37	22	117	59	5225	28	32
18	Haiwee	36	08	117	57	3825	57	58
19	Inyokern	35	39	116	49	2440	30	32
20	Trona	35	46	117	12	1695	60	61
21	Wildrose Ranger Stn	46	16	117	11	4100	15	15
22	Blue Eagle Pch-Hanks	38	32	115	33	4780	04	04
23	Blue Jay HWY Stn	38	23	116	13	5320	19	19
24	Boulder City	35	59	114	51	2525	50	50
25	Caliente	37	37	114	31	4402	55	59
26	Central Nev Field Lab	39	23	117	19	5950	17	17
27	Elgin	37	19	114	30	3300	17	17
28	Logandale Un Exp Farm	36	34	114	28	1320	14	14
29	Valley of Fire St Pk	36	26	114	31	2000	10	10
30	Bishop WSO AP	37	22	118	22	4108	45	68
31	Bodie	38	13	119	01	8370	17	17
32	Independence	36	48	118	12	3950	73	95
33	Mountain Pass	35	28	115	32	4730	22	25
34	White Mountain 2	37	35	118	14	12470	24	24
35	Beowawe U of N Ranch	39	54	116	35	5740	10	10

(a) For explanation of abbreviations used in weather station names refer to NOAA (1981a,b).

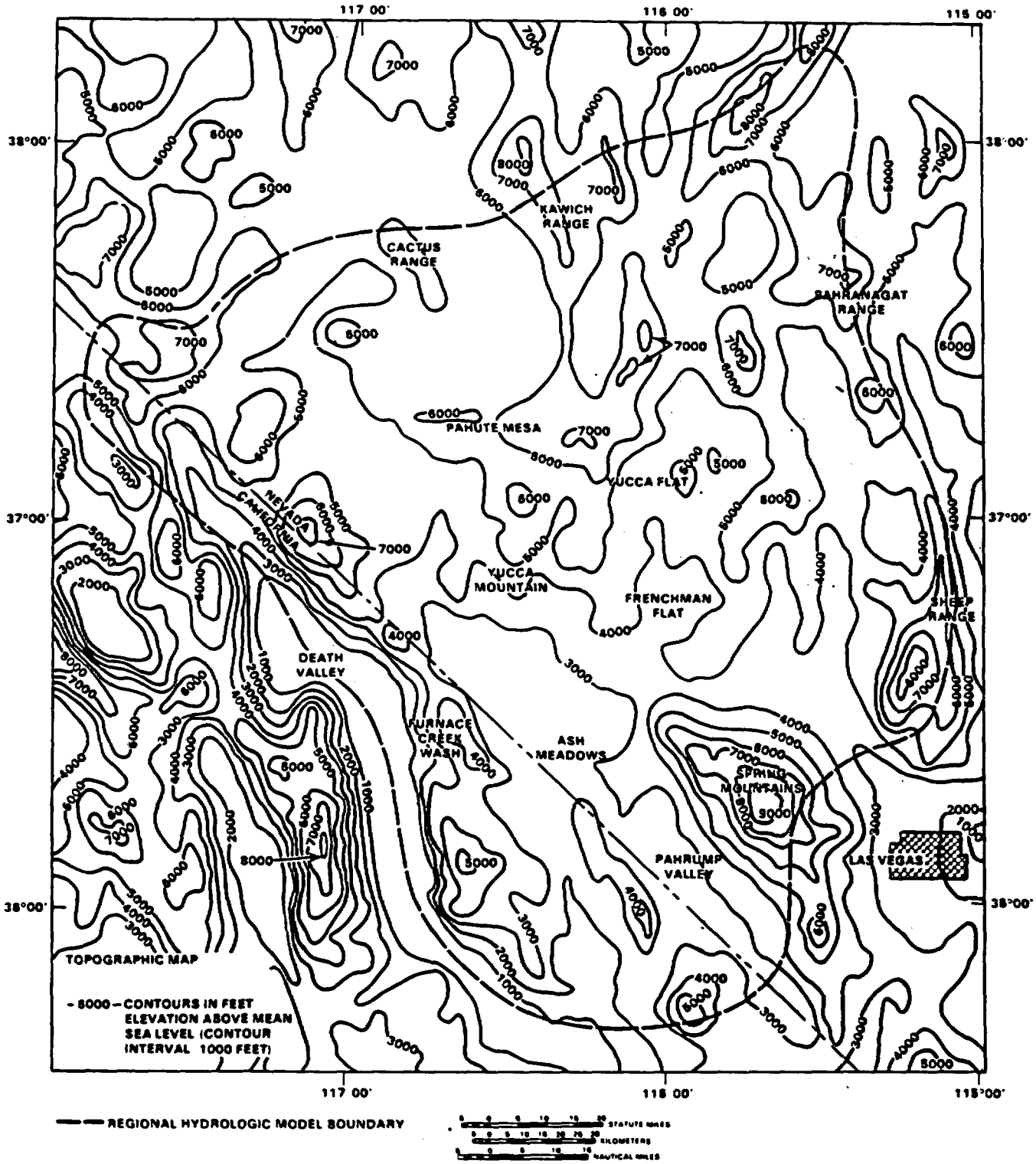

FIGURE A.5. Topographic Distribution for the Regional Model (Elevations in feet above MSL)

necessary climatic measurements needed for more physically based PET models; 2) the predicted error in the Blaney and Criddle method (Blaney and Criddle 1950) of 25% (Doorenbos and Pruitt 1977) is within the error bounds of our final recharge calculation; and 3) the crop coefficient is calculated independently using consumptive use rates of native plant species in southern Nevada.

The Blaney and Criddle formula as stated by Blaney and Criddle (1950) is

$$CU = K(PET_m) = K(p \cdot T/100)$$

where CU = the monthly consumptive use rate of the plant; PET_m = the monthly reference crop potential evapotranspiration; K = a monthly empirical crop coefficient; p = the percentage of total annual daylight hours for the month; and T = the monthly temperature.

Monthly PET was calculated using the period-of-record mean monthly temperature (NOAA 1981a, b) for the 35 weather stations listed in Table A.1 and the monthly percentage of total daylight hours (Table A.2). Monthly PET values were combined into an annual value for each station. Regression of the annual values results in a negative correlation between the logarithm of annual PET and elevation:

$$\log(PET_a) = 1.8 - (7.3 \times 10^{-5})E$$

where PET_a is the annual potential evapotranspiration of the reference crop and E is the weather station elevation in feet above mean sea level. The resulting annual PET distribution is shown in Figure A.6. To fractionalize annual PET distributions to monthly distributions, the mean fraction of annual PET occurring each month for 35 weather stations (see Table A.1) was computed and then normalized. Figure A.7 shows the monthly fraction of PET that was used to calculate monthly PET distributions.

Vegetation

The vegetation distribution assigns a plant type (or species) that is representative of the plant community at each node in the model region. For

TABLE A.2. Monthly Fraction of Annual Hours of Daylight
(from Dunne and Leopold 1978)

Latitude	Jan	Feb	Mar	Apr	May	June	July	Aug	Sept	Oct	Nov	Dec
60°N	0.047	0.057	0.081	0.096	0.117	0.124	0.123	0.107	0.086	0.070	0.050	0.042
50°N	0.060	0.063	0.082	0.092	0.107	0.109	0.110	0.100	0.085	0.075	0.061	0.056
40°N	0.067	0.066	0.082	0.089	0.099	0.100	0.101	0.094	0.083	0.077	0.067	0.075
20°N	0.073	0.070	0.084	0.087	0.095	0.095	0.097	0.092	0.083	0.080	0.072	0.072
10°N	0.081	0.075	0.085	0.084	0.088	0.086	0.089	0.087	0.082	0.083	0.079	0.081
0	0.085	0.077	0.085	0.082	0.085	0.082	0.085	0.085	0.082	0.085	0.082	0.085
10°S	0.098	0.079	0.095	0.081	0.082	0.079	0.081	0.083	0.082	0.086	0.084	0.088
20°S	0.092	0.081	0.086	0.079	0.079	0.074	0.078	0.080	0.081	0.088	0,089	0.093
30°S	0.097	0.083	0.086	0.077	0.074	0.070	0.073	0.078	0.081	0.090	0.092	0.099
40°S	0.102	0.086	0.087	0.075	0.070	0.064	0.068	0.074	0.090	0.092	0.097	0.105

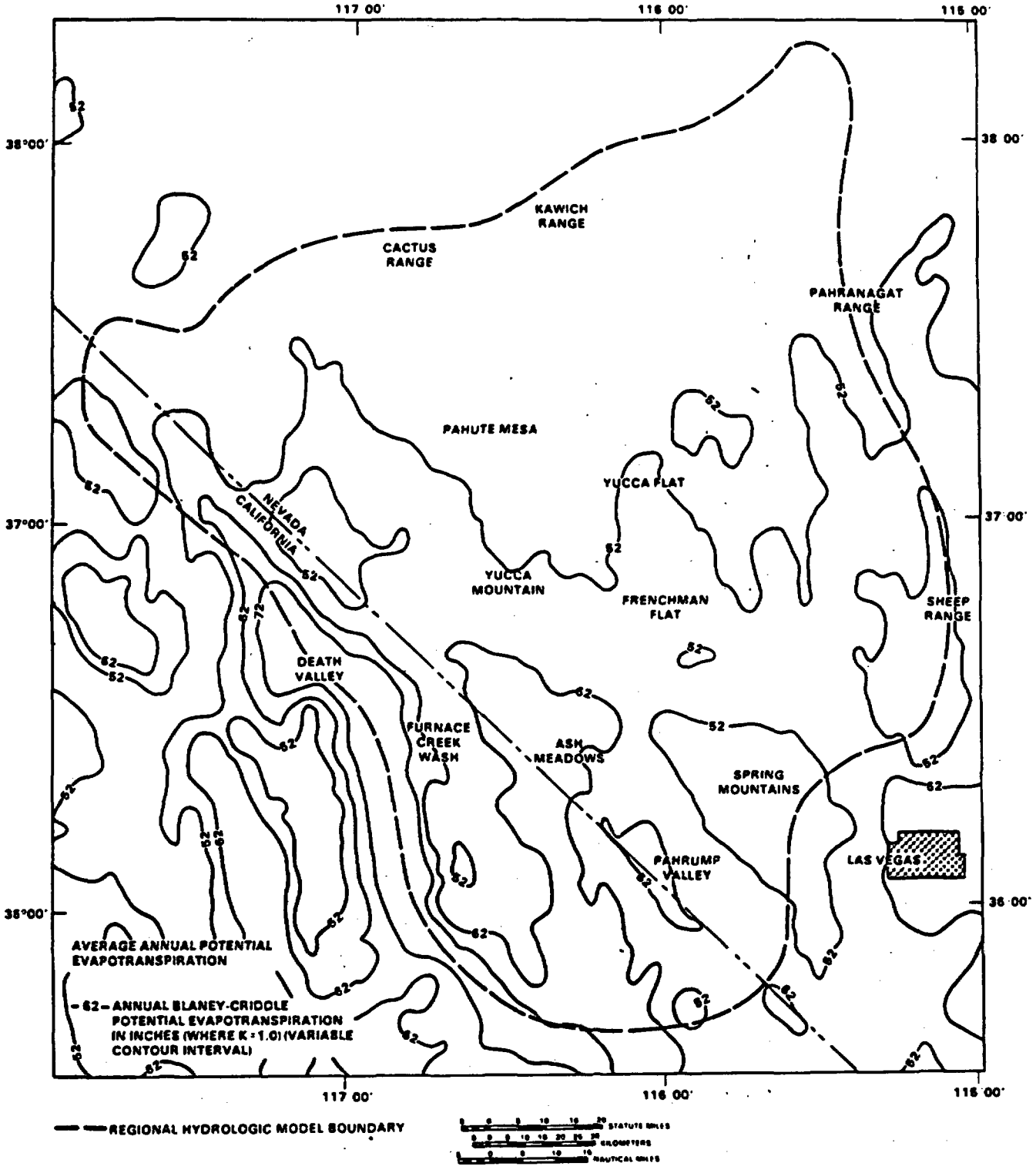

FIGURE A.6. Annual Potential Evapotranspiration Distribution

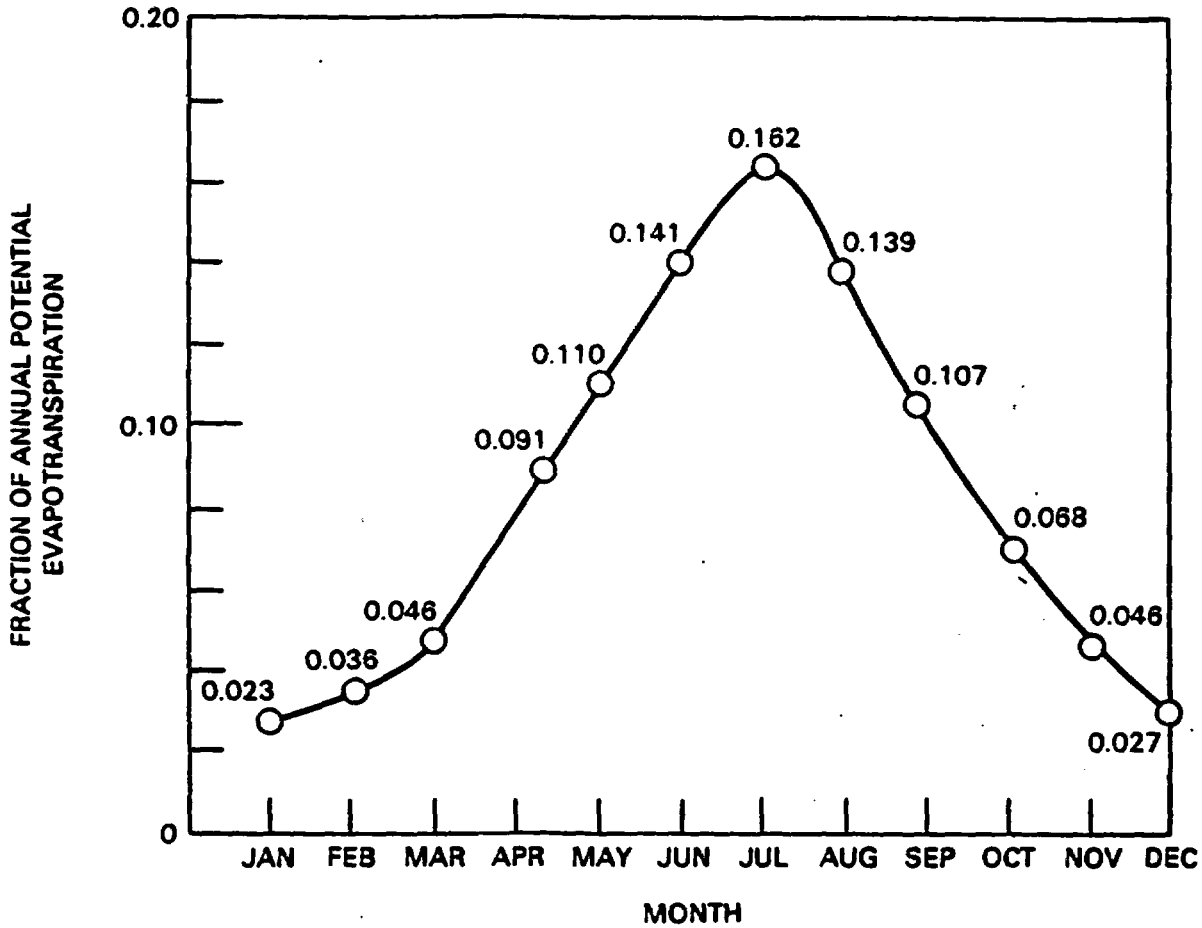

FIGURE A.7. Monthly Fraction of Annual Potential Evapotranspiration used in Calculating Monthly Potential Evapotranspirtation Distributions

each plant type there is a corresponding rooting depth that is used in calculating the available soil water for transpiration and a crop coefficient that is used in computing AET for each plant type from the reference crop PET. The vegetation map is shown in Figure A.8. This map was defined according to the three broad plant communities of the 1) Mojave Desert, 2) Transition Desert, and 3) Great Basin Desert. The plant communities that dominate these deserts are the following: creosote bush, shadscale and greasewood, and sagebrush, respectively (Billings 1949). The criteria for assigning vegetation outlined in Table A.3 provide the required input to construct the vegetation map. A generalized vegetal cover map provided by the Nevada State Engineer's Office (1971b) was used to supplement the guidelines in Table A.3.

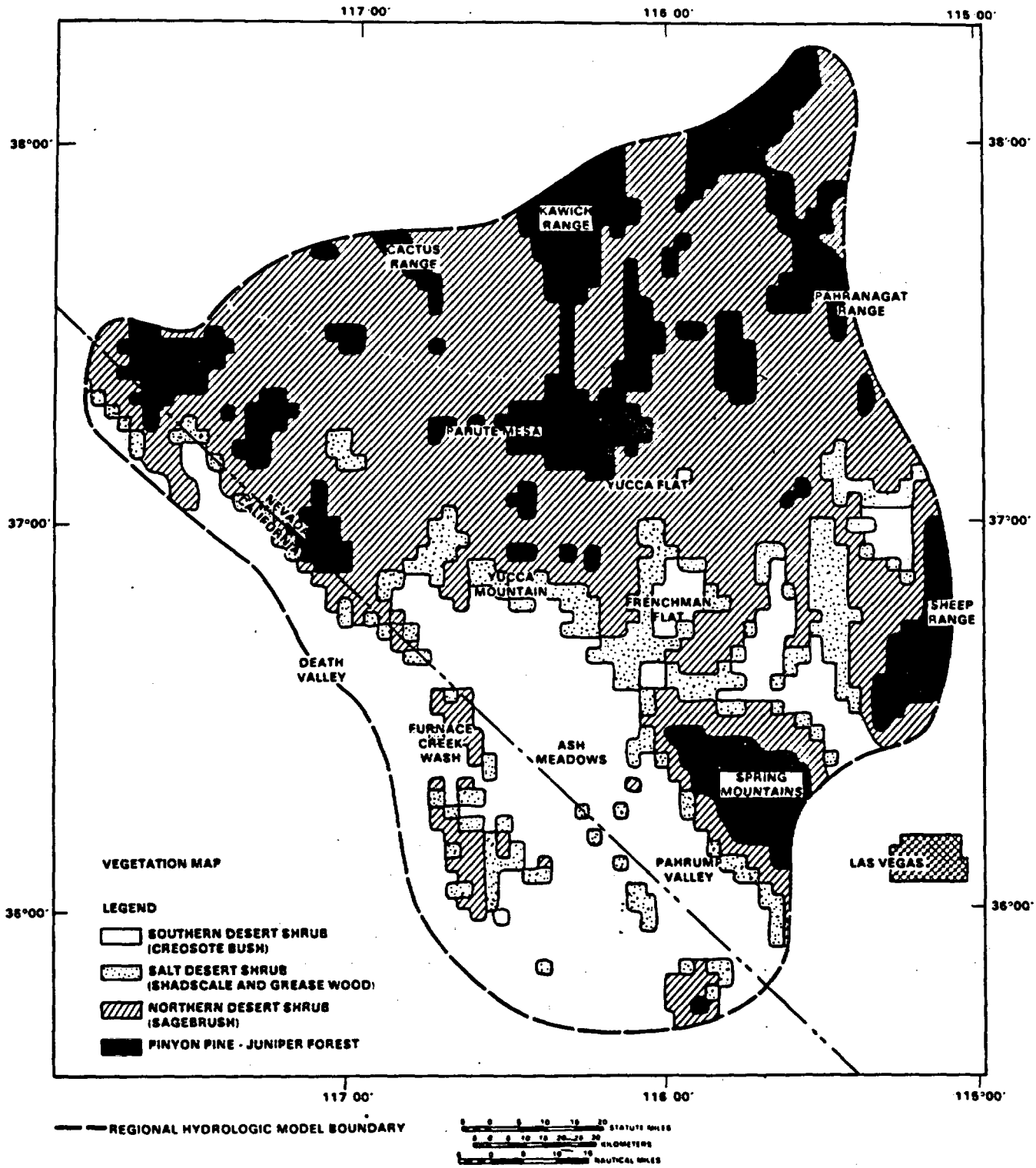

FIGURE A.8. Intrepreted Vegetation Map for the Regional Model

TABLE A.3. Criteria for Vegetation Classification

Desert[a]	Latitude °N	Elevation[b,c] (ft)	Precipitation[b,c] (in./yr)	Plant Type
Mojave Desert	36°-37°	<3500	<6	Creosote bush
		>6000	>10	Pinyon Pine/ Juniper
Transition Desert	37°-38°	<3500	<6	Creosote bush
		4000-5000		Shadscale
		5000-6000	6-10	Sagebrush
		>6000	>10	Pinyon Pine/ Juniper
Great Basin Desert	>37.5°	5000-6000	7-10	Sagebrush
		>6000	>10	Pinyon Pine/ Juniper

(a) From Billings (1949).
(b) From Beatley (1975, 1976).
(c) From Houghton et al. (1975).

Root Zone Depth

The effective root zone depth is that portion of the soil column penetrated by plant roots and, thus, is available for plant transpiration. Mean values of effective root zones are published in the literature. Reported rooting depths for sagebrush are 4.6 feet (Cline, Uresk and Rickard 1977); 5.8 feet (Bramson, Miller and McQueen 1976); 6.4 feet (Campbell and Grant 1977); and 4.5 feet[a].

Reported rooting depths for creosote bush and shadscale are slightly larger: 5.5 feet (Wallace and Rommey 1972) and 5.0 feet[a], respectively.

Rooting depths of pinyon pine and juniper are not available in the literature. Upland soils, however, have a maximum depth of 2.5 feet. Accordingly, the roots of the pinyon pine and juniper were only allowed to penetrate to that soil depth. The mean and range of rooting depths for the plants considered are given in Table A.4.

(a) From unpublished findings on the aerial environment by W. T. Hinds and G. M. Thorp 1982, Pacific Northwest Laboratory, Richland, Washington.

TABLE A.4. Effective Rooting Depths of Native Plants in Southern Nevada

Plant Type	Mean Root Depth (ft)	Range (ft) Minimum	Range (ft) Maximum
Creosote bush	5.0	3.0	6.0
Shadscale	5.0	3.0	6.0
Sagebrush	4.5	3.0	6.0
Pinyon Pine/Juniper	2.5	1.0	3.0

Consumptive Use Crop Coefficient

The crop coefficient, K, of the Blaney and Criddle formula (Blaney and Criddle 1950) is needed to adjust the reference crop PET to reflect the water requirements of a particular plant species. Crop coefficients are usually determined for agricultural crops but not native plant species. However, they may be back-calculated from the Blaney and Criddle formula (Blaney and Criddle 1950) given the consumptive use rate (or actual evapotranspiration) and the reference crop PET because annual evapotranspiration rates are available for creosote bush, sagebrush, and pinyon pine/juniper.

Hinds and Thorp[a] reported an annual evapotranspiration rate of 9.37 inches for semiarid sagebrush/cheatgrass communities of the Arid Lands Ecology (ALE) Reserve located in southeastern Washington. This value is close to the consumptive use rate of 10.7 inches per year reported by Todd (1970) for sagebrush and grassland. By taking the ratio of the consumptive use rate over the reference crop PET for pasture grass, a consumptive use crop coefficient can be evaluated. The ALE and NTS plant communities are similar in ecologic and climatic conditions.[b] Thus, monthly AET was determined from the distribution presented in Figure A.9. The resulting monthly crop coefficients are listed in Table A.5.

(a) From unpublished findings by W. T. Hinds and G. M. Thorp, 1982, Pacific Northwest Laboratory, Richland, Washington.
(b) Personal communication with Dr. W. H. Rickard, Environmental Sciences Department, Pacific Northwest Laboratory, Richland, Washington.

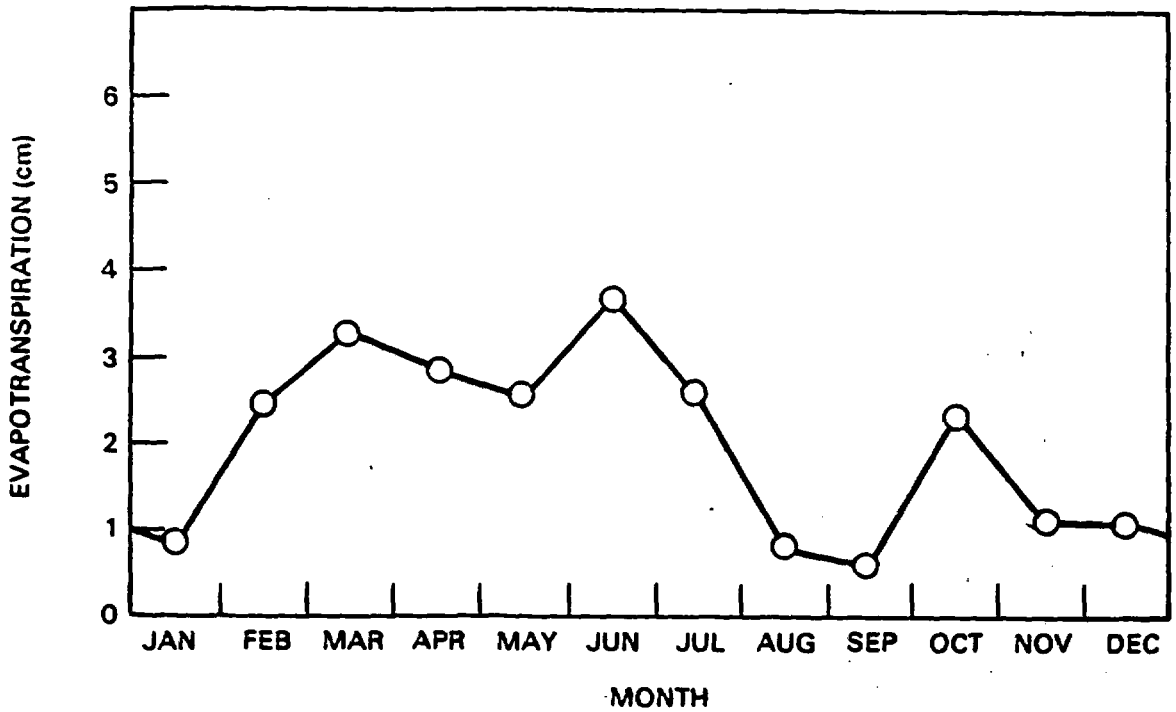

FIGURE A.9. Average Monthly Evapotranspiration at the Arid Lands Ecology ALE Reserve for the Years 1971 to 1974

A similar calculation can be made for the creosote community, given data from Silverbell, Arizona (Evans and Thames 1981). The annual evapotranspiration for creosote bush computed from seasonal rates is 10.8 inches. This value is sufficiently similar to the evapotranspiration rate for sagebrush for these crop coefficients to be applied to creosote bush. Again, the unavailability of consumptive use rates for shadscale makes it necessary to also substitute sagebrush consumptive use rates for this plant.

Todd (1970) reports the annual evapotranspiration for pinyon pine/juniper as 14.5 inches. The monthly consumptive use crop coefficients were computed by fractionalizing the annual consumptive use rate into monthly values given the distribution of monthly evapotranspiration distribution for a typical pine forest, and then taking the ratio of these values over the reference crop monthly consumptive use rate. The resulting monthly values are listed in Table A.5.

TABLE A.5. Monthly Blaney and Criddle Crop Coefficient (Blaney and Criddle 1950) for Major Plant Types of the Model Region

Plant Type	Jan	Feb	Mar	Apr	May	June	July	Aug	Sept	Oct	Nov	Dec
Creosote bush	1.60	3.46	1.70	0.52	0.25	0.28	0.16	0.06	0.06	0.06	1.26	1.96
Shadscale	1.60	3.46	1.70	0.52	0.25	0.28	0.16	0.06	0.06	0.06	1.26	1.96
Sagebrush	1.60	3.46	1.70	0.52	0.25	0.28	0.16	0.06	0.06	0.06	1.26	1.96
Pinyon Pine/ Juniper	0.507	0.502	0.466	0.478	0.479	0.478	0.478	0.479	0.479	0.48	0.469	0.461

Soil

The calculation of AET by conventional means requires the available water-holding capacity for each soil. The available water-holding capacity is the water available in a soil for plant transpiration. Soil type must be first assigned at each node in the hydrologic model so that the available water-holding capacity associated with each soil type can be designated. Soil types were assigned according to the major landforms found in the Basin and Range physiographic province as designated by Peterson (1981). A bibliography of the soil surveys consulted to identify the available water-holding capacity of soils associated with the major landforms can be found at the end of this appendix. The land slopes listed in Table A.6 were used to identify each landform and to assign soil types and their available water-holding capacity. The resulting soil distribution is displayed in Figure A.10.

Soil Root-Zone Water-Holding Capacity

The root-zone depth (inches) for each vegetation type (see Table A.4) multiplied by available water-holding capacity (inches/inch) of soil (Table A.6) gives the soil root-zone water-holding capacity in inches (Table A.7). Actual evapotranspiration is a function of the moisture status of the soil, which, in turn, is dependent on the soil root-zone water-holding capacity. Recharge occurs only when the soil moisture status is in excess of the soil root-zone water-holding and runoff.

Runoff

Annual runoff is another parameter used in the recharge calculation (see the equation for recharge). An annual runoff map for the state of Nevada was obtained from the Nevada State Engineer's Office (1971a) and digitized (Figure A.11).

ACTUAL EVAPOTRANSPIRATION CALCULATION SEQUENCE

Actual evapotranspiration may be calculated from PET by a number of schemes reported in the literature. The status of soil moisture is used in most relationships. The Thornthwaite and Mather (1955) linear relationship was used to determine AET for the regional model. The Thornthwaite and Mather

TABLE A.6. Available Water Holding Capacity for Soils of the Major Landforms of the Model Region

Soil Type	Landform	Land Slope	Soil Depth (in.)	Available Water-Holding Capacity of Soil (in./in.)
1	Playa/flood Plains	≤0.6%	0 - 24	0.14 - 0.17
			24 - 60	0.15 - 0.18
2	Alluvial apron	0.6 - 4%	0 - 9	0.14 - 0.17
			9 - 60	0.17 - 0.19
3	Alluvial fan	4 - 8%	0 - 2	0.04 - 0.08
			2 - 19	0.08 - 0.15
			19 - 60	0.05 - 0.07
4	Mountains/ foothills	>8%	0 - 17	0.05 - 0.07
			17 - 30	0.08 - 0.10

relationship states that the rate of AET is equal to the PET times the ratio of the antecedent soil moisture conditions (i.e., the amount of moisture in the soil) over the soil root-zone water-holding capacity.

Estimation of Recharge

The estimation of aquifer recharge is based on a monthly time step and is performed at each node of the regional hydrologic model. Estimates of monthly precipitation and Blaney and Criddle PET (Blaney Criddle 1950) were made from weather station data previously described and then interpolated to each model node using regression equations. The estimates of PET were converted to consumptive use rates given the crop coefficients listed in Table A.5; and the vegetation type designated in Figure A.8. The root-zone water-holding capacity (Table A.7) was determined from the vegetation (see Fig. A.8) and the soil type (see Fig. A.10) at a given node.

The calculation of AET by the Thornthwaite and Mather (1955) method depends on the status of the soil moisture. However, because this is unknown our AET calculations assume an initial soil moisture on January 1 of 1 inch less than the soil root-zone water-holding capacity. An iterative procedure is then used to evaluate a mean monthly AET and recharge value. These values are calculated by allowing the AET calculation to cycle yearly until the soil

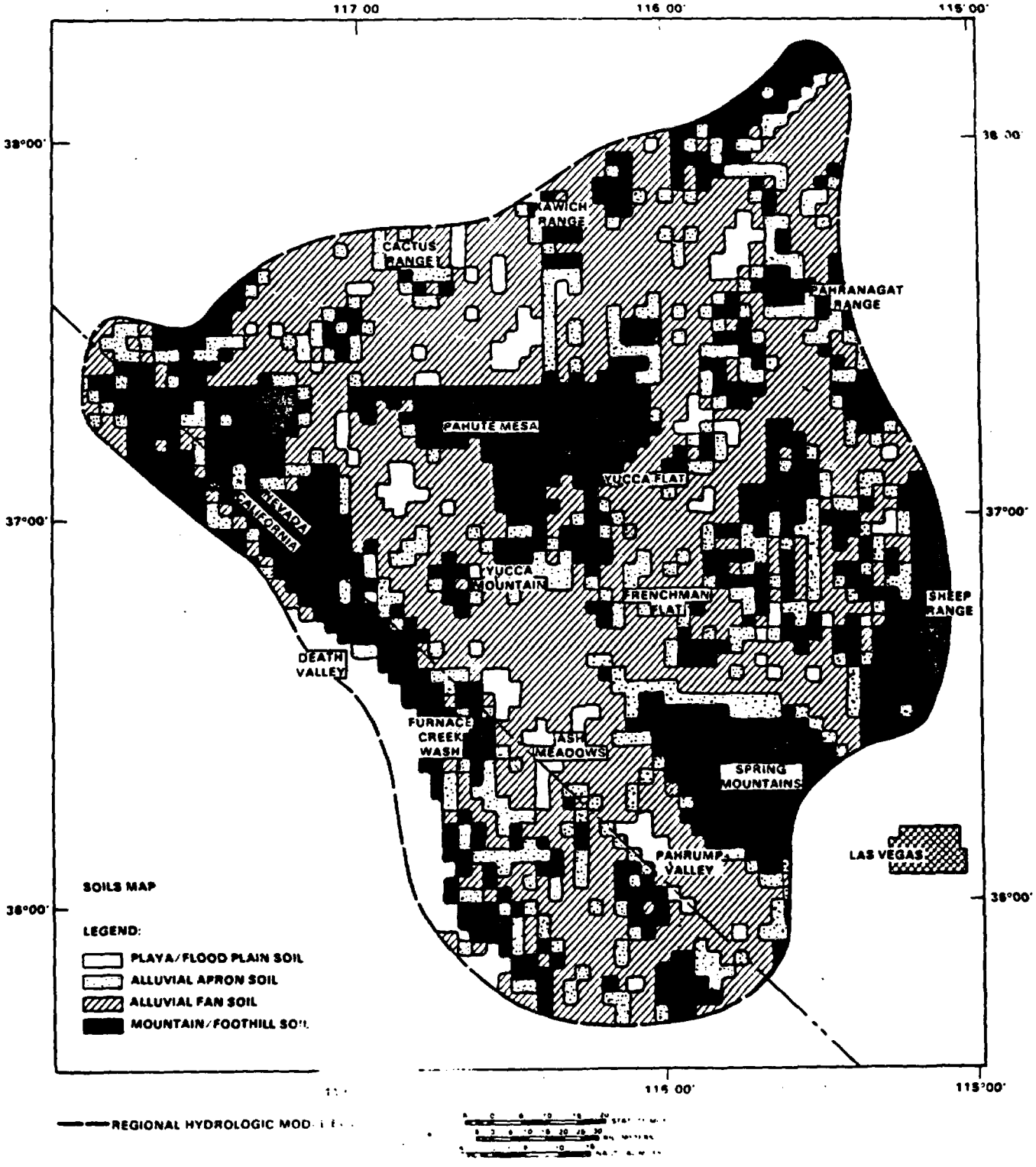

FIGURE A.10. [illegible] for the Regional Model

TABLE A.7. Soil Root-Zone Water-Holding Capacity (in.), as a Function of Soil and Plant Type

Soil Type	Plant Type			
	Creosote Bush	Shadscale	Sagebrush	Pinyon Pine/ Juniper
Playa/Flood Plain	9.6	9.6	8.4	4.8
Alluvial Apron	10.6	10.6	9.5	5.2
Alluvial Fan	4.6	4.6	4.2	2.8
Mountains/Foothills	2.2	2.2	2.2	2.2

moisture content on December 31 is the same (i.e., within a convergence criteria of 0.01) as the moisture content at the beginning of the year on January 1. When this convergence has occurred, the soil moisture status has achieved a cyclic steady-state condition. The values that are calculated for AET and recharge under these soil moisture conditions are then mean values for cyclic steady-state conditions.

The results of such an AET and recharge calculation for a typical node with a plant type of pinyon pine/juniper are presented in Table A.8. Annual recharge is obtained by subtracting the annual runoff from the recharge plus runoff column.

Appendix C presents a detailed explanation of the iterative procedure that will clarify how the values in Table A.8 are obtained. Table C.1 of Appendix C shows the soil moisture content converging to its cyclic steady-state value, while Table C.2 presents hand calculations of the water balance used in calculating recharge for one month.

Discussion of Results

The resulting recharge distribution is shown in Figure A.12. The total recharge for this distribution is 9.99×10^4 acre-feet per year. Generally, recharge occurs in mountainous areas where there is winter snowpack. Two additional criteria for recharge become evident by comparing the recharge distribution (see Fig. A.12) with the precipitation and topography distributions (see Fig. A.3 and A.5, respectively). Recharge occurs if the elevation is greater than 5,500 feet and the annual precipitation is greater than

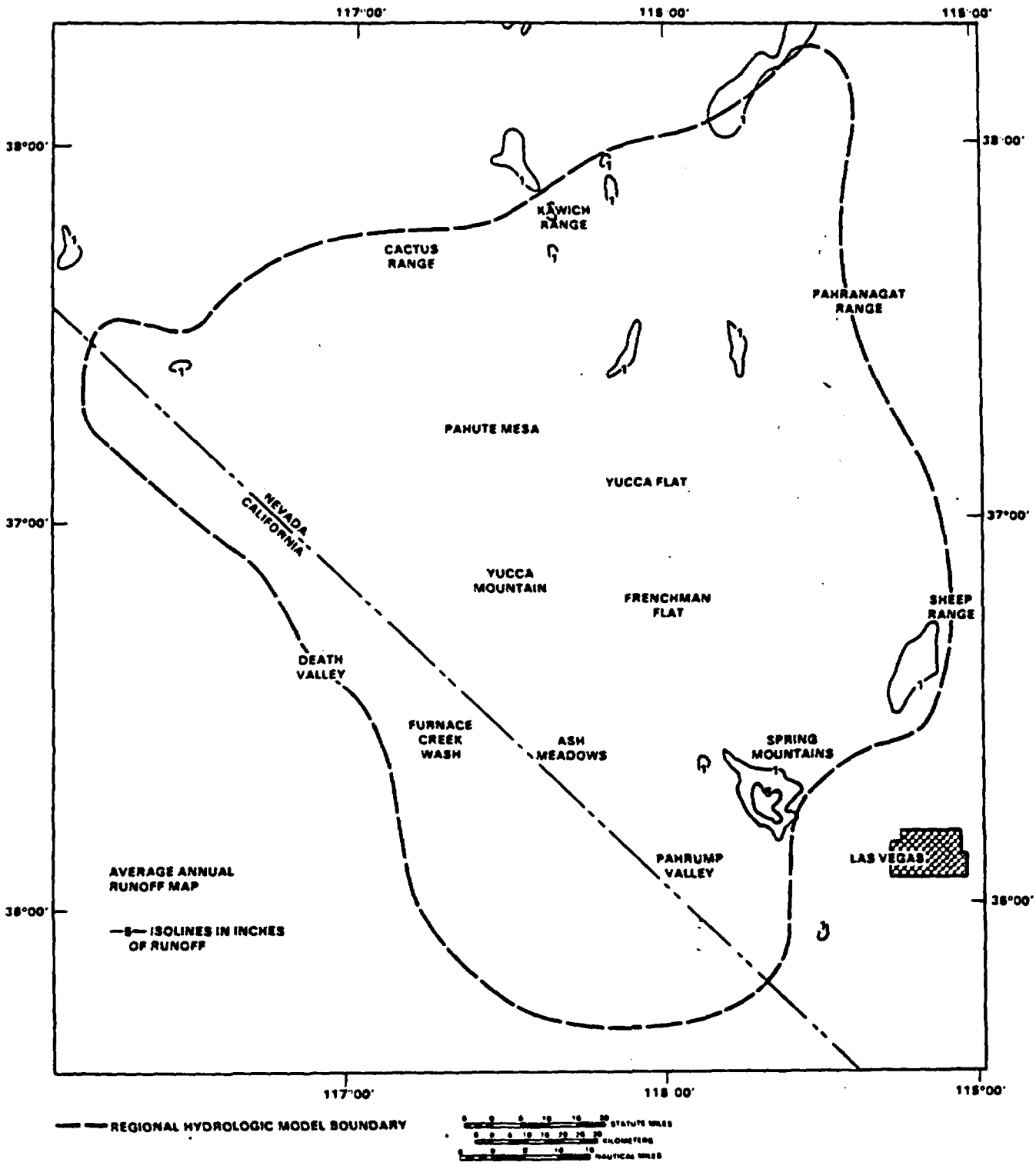

FIGURE A.11. Annual Runoff Map for the Model Region (after Nevada State Engineer's Office 1971a)

TABLE A.8. Example Results from Calculation of Actual Evapotranspiration on a Monthly Basis for a Typical Pinyon Pine/Juniper Node

Pinyon Pine Juniper Node:

Node location: near the base of the Spring Mountains
Plant type: pinyon pine/juniper
Soil type: mountains/foothills

Month	Rainfall (in.)	PET (in.)	AET (in.)	Soil Moisture (in.)	Recharge Plus Runoff (in.)
January	1.6327	0.5968	0.5968	1.7547	0.0000
February	1.8801	0.7597	0.7597	2.2000	0.6751
March	2.9686	0.9011	0.9011	2.2000	2.0674
April	1.3194	1.8285	1.8285	1.6908	0.0000
May	2.1390	2.2150	2.1974	1.6325	0.0000
June	0.0990	2.8132	1.7314	0.0000	0.0000
July	0.6762	3.2552	0.6762	0.0000	0.0000
August	1.3804	2.8190	1.3804	0.0000	0.0000
September	0.9730	2.1545	0.9730	0.0000	0.0000
October	1.2188	1.3664	1.2188	0.0000	0.0000
November	1.4398	0.9069	0.9069	0.5328	0.0000
December	0.7092	0.5232	0.5232	0.7188	0.0000

Annual rainfall = 16.44 in.
Annual PET = 20.14 in.
Annual AET = 13.69 in.
Annual runoff = 0.00 in.
Annual recharge = 2.74 in.

10.0 inches. These two criteria meet the plant requirements of pinyon pine and juniper (see Table A.3). It is also evident by examining Table A.8 that recharge occurs during the early spring months when the winter snowpack melts and seeps into the ground.

The initial estimate for recharge of 9.99×10^4 acre-feet per year is sensitive to various parameters used in the calculation of AET. Two such

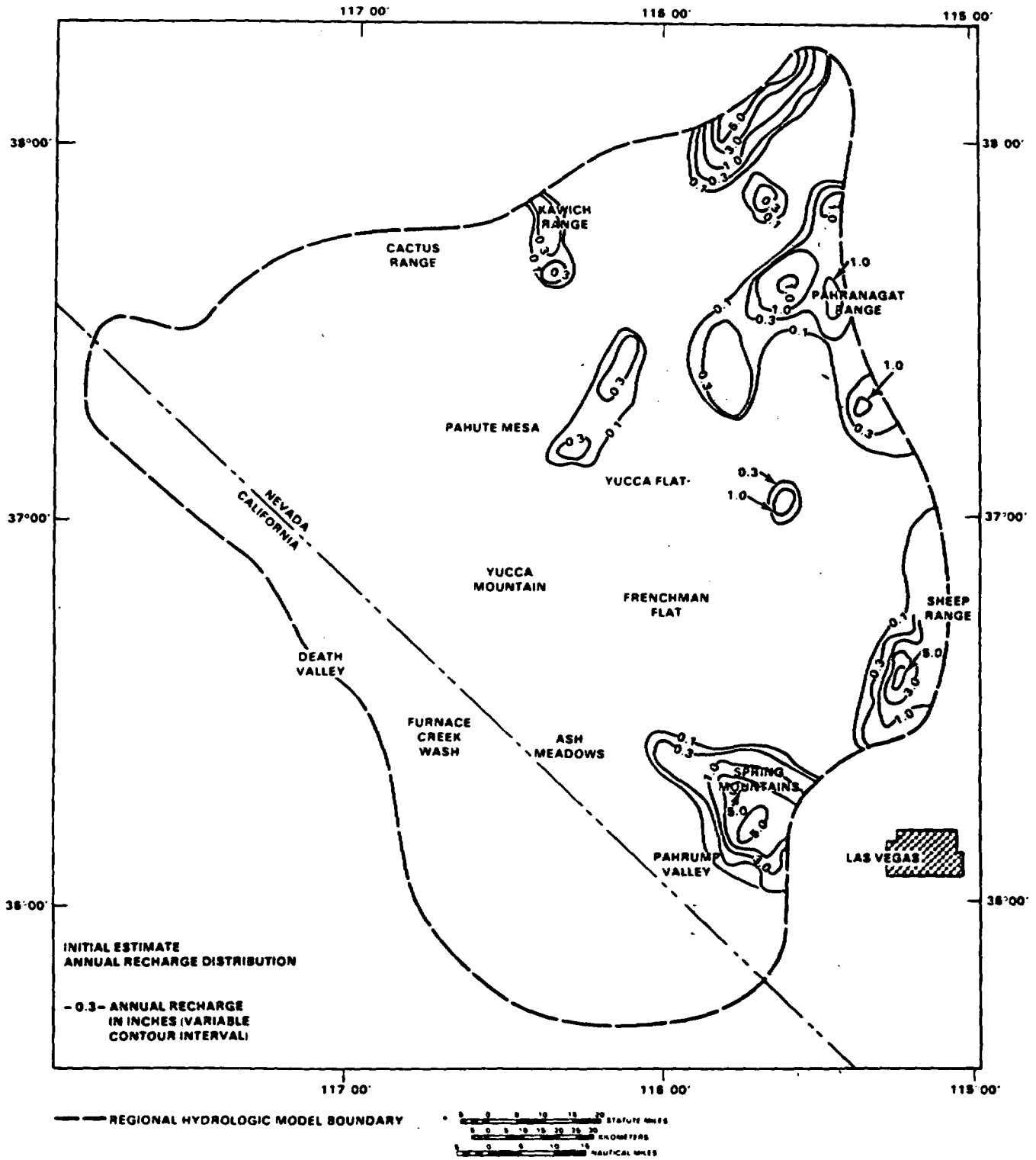

FIGURE A.12. Initial Estimate of Recharge Distribution

parameters are plant root-zone depth and Blaney and Criddle crop coefficient (Blaney and Criddle 1950). These two parameters were examined in a sensitivity analysis to determine the plausible range in recharge given the uncertainty in these parameters. From these studies, the best estimate of recharge was selected for use in calibrating the hydrologic model.

RECHARGE SENSITIVITY ANALYSIS

Two parameters that are not well documented in the literature are plant rooting depths and consumptive use crop coefficients. Sensitivity of the recharge calculation to each parameter is discussed below.

The soil root-zone water-holding capacity is a function of plant root depth (see Table A.7) and determines that portion of the soil water available for plant transpiration. The range in rooting depths for each plant type is given in Table A.4. The minimum rooting depth was used in the recharge sensitivity analysis to determine an upper bound on the recharge estimate.

The Blaney and Criddle crop coefficient (Blaney and Criddle 1950) is even more sensitive and will therefore provide greater uncertainty to the recharge estimate than plant rooting depth. Calculations show that recharge occurs only at elevations where pinyon pine or juniper grow. Consequently, the analysis is focused on varying the pinyon pine/juniper crop coefficient.

Results

Table A.9 gives the results of the sensitivity analysis when both plant rooting depths and consumptive use crop coefficients are varied. The consideration of other crop coefficients (i.e., grapes, olives, and peaches) tends to reduce recharge by increasing the consumptive use of available moisture. The recharge estimates presented in Table A.9 bracket recharge between 5.36×10^4 acre-feet per year and 2.14×10^5 acre-feet per year. Recall that the initial recharge estimate is 9.99×10^4 acre-feet per year.

To determine which estimate of recharge to use in the regional model, two additional factors were considered. First, the distribution of recharge should agree with the areal distribution of winter snowpack. Second, the assumptions concerning runoff should be stated. Storm runoff in southern Nevada occurs in

TABLE A.9. Sensitivity of Recharge Estimates to Variations in Soil Water Capacity and Consumptive Use Crop Coefficient (K)

Plant Type	Recharge Estimate (acre-ft/yr) Mean Root Depth[a]	Minimum Root Depth[a]
Pinyon pine/juniper (K)[b]	9.97×10^4	2.14×10^5
Grapes (drywind; 30% cover) (K)[c]	5.72×10^4	1.32×10^5
Olives (K = 0.4/month)[c]	7.70×10^4	1.56×10^5
Peaches (dry strong wind) (K)[c]	5.36×10^4	1.32×10^5

(a) Reference Table A.4.
(b) Reference Table A.5.
(c) Reference Doorenbos and Prutt (1977).

ephemeral streams, which may recharge the ground water. If we assume that evaporative losses during runoff are zero, then all runoff will recharge the ground water resulting in an approximately 30% increase in recharge. The total recharge for this distribution is 1.33×10^5 acre-feet per year and is presented in Figure A.13. This distribution allows more recharge to occur on Pahute Mesa consistent with recent winter LANDSAT imagery showing snowpack on the mesa. The distribution of recharge shown in Figure A.13 is considered to be the best estimate of recharge.

Sass and Lachenbruch (1982) estimate an average verticle flux at Yucca Mountain through the unsaturated zone and upper saturated zone of 8 millimeters per year (0.32 inches per year). The recharge distributions determined by our sensitivity analysis show no recharge occurring at Yucca Mountain. The conclusion is that recharge calculations in this study are made at too gross a scale to compute the small amount of recharge occurring at this site.

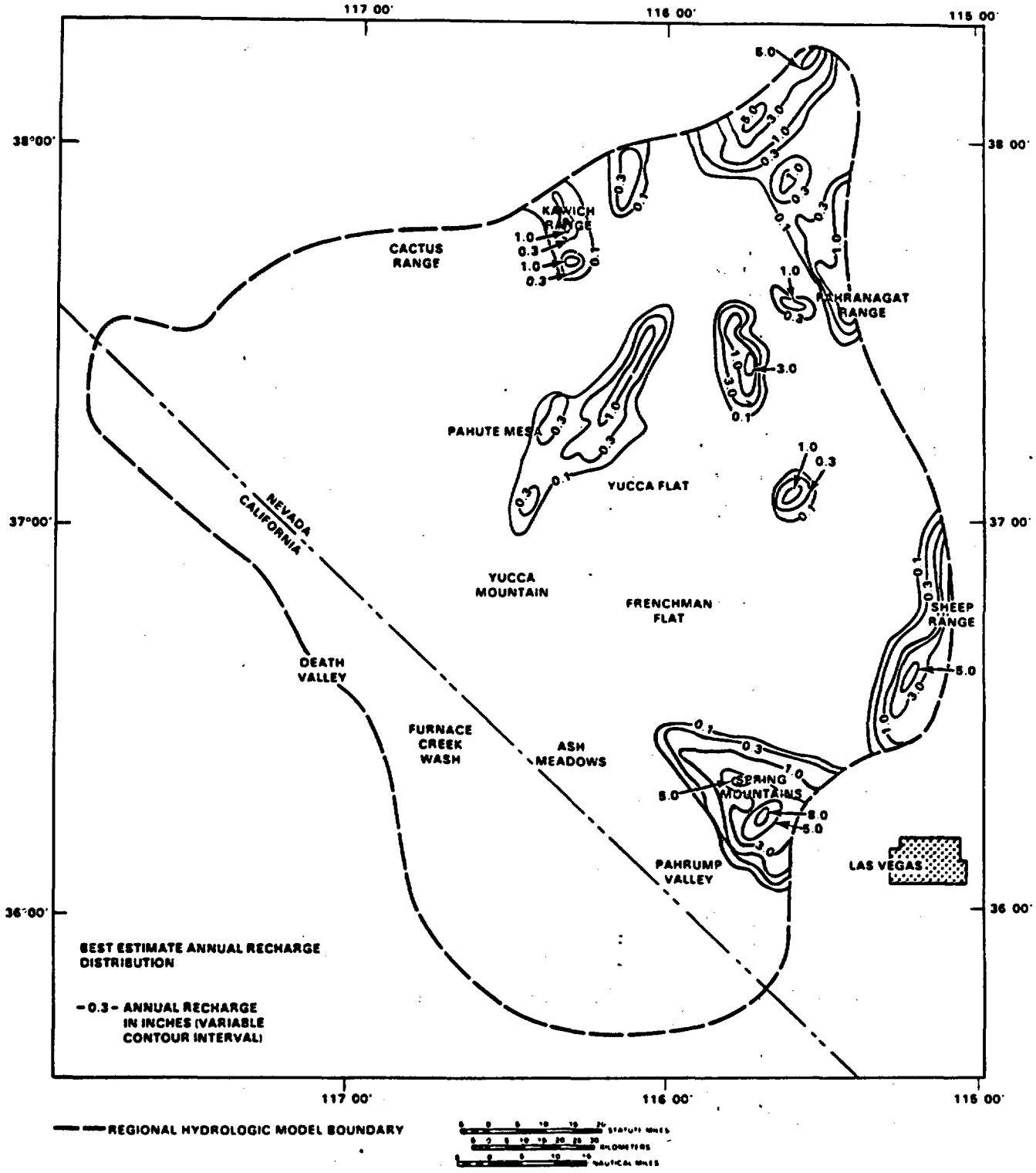

FIGURE A.13. Best Estimate of Recharge Distribution

REFERENCES

Blaney, H. F. and W. D. Criddle. 1950. "Determining Water Requirements in Irrigated Areas from Climatological and Irrigation Data." USDA(SCS). TP-96.

Beatley, J. C. 1975. "Climatic and Vegetation Pattern Across the Mojave/Great Basin Desert Transition of Southern Nevada." Am. Midland Naturalist. 93(1):53-70.

Beatley, J. C. 1976. Vascular Plants of the Nevada Test Site and Central-Southern Nevada: Ecological and Geographical Distributions. TID-26881. Laboratory of Nuclear Medicine and Radiation Biology, University of California, Davis, California.

Billings, W. D. 1949. "The Shadscale Vegetation Zone of Nevada and Eastern California in Relation to Climate and Soils." Am. Midland Naturalist. 42(1):87-109.

Bramson, F. A., R. F. Miller and I. S. McQueen. 1976. "Moisture Relationships in Twelve Northern Desert Shrub Communities Near Grand Junction, Colorado." Ecology 57(6):1104-1124.

Campbell, G. S. and G. A. Grant. 1977. "Water Relations and Water Use Patterns for Armtemisia Tridentata Nutt. in Wet and Dry Years," Ecology 58(3):652-659.

Cline, J. F., I. W. Uresk, and W. H. Rickard. 1977. "Comparison of Soil Water Used by a Sagebrush-Bunchgrass and a Cheatgrass Community." J. Range Management 30(3):199-201.

Doorenbos, G. and W. O. Pruitt. 1977. "Guide Lines for Predicting Crop Water Requirements." In Irrigation and Drainage Paper 24, 2nd edition. Food and Agricultural Organization of the United Nations, Rome.

Dunne, T. and L. B. Leopold. 1978. Water in Environmental Planning. W. H. Freeman & Company, San Francisco, California.

Evans, D. D. and G. L. Thames, eds. 1981. Water in Desert Ecosystems. Dowden, Hutchinson, and Ross, Inc., Stroudsburg, Pennsylvania.

French, R. H. 1983. "Precipitation in Southern Nevada." J. Hydraulic Engineering (ASCE), 109(7):1023-1036.

Houghton, J. G., C. M. Sakamoto and R. O. Gifford. 1975. Nevada's Weather and Climate. Special Publication 2. Nevada Bureau of Mines and Geology, University of Nevada, Reno, Nevada, 78 p.

NOAA (National Oceanic and Atmospheric Administration) Environmental Data Service. 1981a. Climatic Data Annual Summary, Nevada. National Climatic Center, Asheville, North Carolina.

NOAA (National Oceanic and Atmospheric Administration) Environmental Data Service. 1981b. Climatic Data Annual Summary, California. National Climatic Center, Asheville, North Carolina.

Nevada State Engineer's Office. 1971a. Water for Nevada Hydrologic Atlas. Map S-4: Average Annual Runoff Map. University of Nevada, Reno, Nevada.

Nevada State Engineer's Office. 1971b. Water for Nevada Hydrologic Atlas. Map S-12: Vegetal Cover Map. University of Nevada, Reno, Nevada.

Peterson, F. F. 1981. Landforms of the Basin and Range Province Defined for Soil Survey. Nevada Agricultural Bulletin No. 28, Max C. Fleischmann College of Agriculture, University of Nevada, Reno, Nevada.

Quiring, R. F. 1965. Annual Precipitation Amount as a Function of Elevation in Nevada South of 38 1/2 Degrees Latitude. Weather Bureau Research Station, Las Vegas, Nevada.

Sass, G. H. and A. H. Lachenbruch. 1982. Preliminary Interpretation of Thermal Data from the Nevada Test Site. U.S. Geol. Surv. Open-File Report (in review).

Thornthwaite, L. W. and G. R. Mather. 1955. The Water Balance. Laboratory of Climatology, Publication No. 8, Centerton, New Jersey.

Todd, D. K., ed. 1970. The Water Encyclopedia. Water Information Center, Port Washington, New York.

Wallace, A. and E. M. Rommey. 1972. Radioecology and Ecophysiology of Desert Plants at the Nevada Test Site. TID-25954, Environmental Radiation Division, Laboratory of Nuclear Medicine and Radiation Biology and Agricultural Sciences, Los Angeles, California.

BIBLIOGRAPHY OF SOIL SURVEYS

The soil surveys that were consulted to determine the water-bearing properties of soils in the study area are listed below:

Archer, W. M. 1980. Soil Survey of Diamond Valley Area Parts of Eureka, Elko, and White Pine Counties, Nevada. U.S. Department of Agriculture, Soil Conservation Service.

Candland, D. M. 1980. Soil Survey of Big Smokey Valley Area, Nevada, Part of Nye County. U.S. Department of Agriculture, Soil Conservation Service.

Langan, L. N. and L. I. Larsen. 1967. Soil Survey of Las Vegas and El Dorado Valleys Area, Nevada. No. 23:1957. U.S. Department of Agriculture, Soil Conservation Service.

Leavitt, V. D. 1970. Soil Survey of Area 18, Nevada Test Site. Report SWRHL-74r, Southwest. Radiological Health Laboratory, Las Vegas, Nevada.

Leavitt, V. D. and B. J. Mason. 1971. Soil Survey of Area 15, Nevada Test Site. Report SWRHL-106r. Southwest Radiological Health Laboratory, Las Vegas, Nevada.

Leavitt, V. D. 1974. Soil Surveys of Five Plutonium Contaminated Areas on the Test Range Complex in Nevada. NERC-2V-539-28, Environmental Protection Agency, Las Vegas, Nevada.

Leavitt, V., G. Garlick, G. Woodruff and D. Bagley. 1980. Soil Survey of Virginia River Area, Nevada-Arizona and Part of Mohave County, Arizona. U.S. Department of Agriculture, Soil Conservation Service.

APPENDIX B

DISCHARGE CALCULATION SUMMARY TABLES

TABLE B.1. Reference Sources used in the Discharge Calculation for the Nevada Test Site Regional Model

Referral Letter	Reference	Source
A	Harrill, James R., 1982. Ground-Water Storage and Depletion in Pahrump Valley, Nevada-California 1962-1975. USGS Open-File Report 81-635.	- Figure 9-Distribution of pumpage in 1975 - Plate 3D-Simulated distribution of evapotranspirtation, 1976
B	Pistrang, M. A. and F. Kunkel. 1964. A Brief Geologic and Hydrologic Reconnaissance of the Furnace Creek Wash Area, Death Valley National Monument, California. USGS Water Supply Paper 1779-Y.	- Table 4-Total estimated rate of ground-water discharge in 1956-57 in the Furnace Creek Wash Area
C	Dudley, W. W. and J. D. Larsen. 1975. Effects of Irrigation Pumping on Desert Pupfish Habitats In Ash Meadows, Nye County, Nevada. USGS Prof. Paper No. 927.	
D	Bateman, R. L., A. L. Mindling, R. L. Naff and H. M. Joung. 1972. Development and Management of Groundwater and Related Environmental Factors in Arid Alluvial and Carbonate Basins in Southern Nevada. Desert Research Institute Project Report No. 18, Reno, Nevada.	- Appendix B-Groundwater Rights, Ask Meadows Sub-Basin, Nye County, Nevada
E	Winograd, I. Z. and W. Thordarson. 1975. Hydrogeologic and Hydrochemical Framework, South Central Great Basin, Nevada-California, with Special Reference to the Nevada Test Site. USGS Prof. Paper 712-C.	- Plate 1-Hydrogeologic map of Nevada Test Site and vicinity, Southern Nevada
F	White, A. F. 1979. Geochemistry of Groundwater Associated with Tuffacious Rocks, Oasis Valley, Nevada. USGS Prof. Paper 712-E.	

TABLE B.1. (Contd)

Referral Letter	Reference	Source
G	Rush, R. E. 1968. Water Resources Appraisal of Clayton Valley - Stonewall Flat Area, Nevada and California. Nevada Department of Conservation and Natural Resources, Water Resources Reconnaissance Series Report No. 45.	- Table 8-Estimated average and annual evapotranspiration of ground water - Table 9-Summary of Estimated Net Well Pumpages in 1966 - Table 15-Selected springs data
H	Thordarson, W. and B. P. Robinson. Wells and Springs in California and Nevada Within 100 Miles of the Point 37°15' N and 116°25' W on the Nevada Test Site. U.S. Geol. Surv. Report 474-85, 174 p.	
I	Winograd, I. G. 1963. A Summary of the Groundwater Hydrology of the Area Between the Las Vegas Valley and the Amargosa Desert, Nevada. USGS Water Supply Paper TEI-840.	
J	Walker, G. E. and T. E. Eakin. 1963. Geology and Groundwater of Amargosa Desert, Nevada - California. Nevada Department of Conservation and Natural Resources, Water Resources Reconnaissance Series Report No. 14.	- Table 7-Estimated Average Annual ground-water discharge by natural processes from the Amargosa Desert, Nevada - California
K	Hunt, C. B., T. W. Robinson, W. A. Bowles and A. L. Washburn. 1966. Hydrologic Basin, Death Valley, California. USGS Prof. Paper 494-B.	- Table 25-Summary of ground-water discharge in Death Valley by areas

TABLE B.2. Summary of Sources Referenced for the Discharge Calculation by Geographic Location

Geographic Location	Pumping	Discharge Springs	Evapotranspiration
Pahrump Valley	Reference A - Figure 9	Reference A - Figure 9	Reference A - Plate 3D
Furnace Creek	Reference B - Plate 1 and Table 4	Reference B - Plate 1 and Table 4	Reference B - Plate 1 and Table 4
Ash Meadows	Reference C - p. 22 Reference D - p. 37	Reference C - p. 12 Reference D - p. 38	Reference E - Plate 1
Pahute Mesa (Oasis Valley)			Reference E - Plate 1 Reference F - p. 6
Alkali, Clayton, and Lida Valleys and Oriental Wash	Reference G - Table 9	Reference G - Table 15 and p. 31-32	Reference G - Table 8
Three Lakes and Indian Springs Valley	Reference I - p. 23	Reference H - p. 160	Reference J - Table 7 Reference E - Plate 1
Amargosa Desert (Alkali Flat and Sarcobatus Flat)			Reference J - Table 7 Reference E - p. C84 Reference E - Plate 1
Death Valley		Reference K - Table 25	Reference K - Table 25 Reference J - Table 7

TABLE B.3. Discharging Nodes for the Regional Model by Geographic Location

Geographic Location	Line	Column	Discharge (ft^3/day/Node)
Spring and Pumping Discharges per Node			
Pahrump Valley	16	47, 48	2.014×10^5
	17	47, 48, 49	2.014×10^5
	18	44, 45, 46, 47, 48	2.014×10^5
	19	45, 46	2.014×10^5
	20	44, 45, 46	2.014×10^5
	21	46	2.014×10^5
	22	45, 46	2.014×10^5
Furnace Creek Wash Area			
Texas and Travetine Springs	26	27	4.06×10^5
Nevada Springs	28	27	6.047×10^4
Ash Meadows	23	39, 40	3.31×10^5
	24	39, 40	3.31×10^5
	25	39	8.25×10^5
	26	38, 39	8.25×10^5
	27	38, 39	7.94×10^5
Grapevine Springs	45	14	1.19×10^4
Straininger Springs	45	15	7.16×10^3
Stonewall Flat Area			
Ralston	56	19	1.19×10^3
Lida Valley Junction	58	19, 20	0.597×10^3
Oriental Wash	51	11	1.19×10^3
Goldfield Area	62	18	4.77×10^3
	63	21	3.35×10^3
Three Lakes Valley	25	61	2.39×10^4
Indian Spring Valley	29	54	8.38×10^4
Sand Spring Valley	60	49	2.00×10^5
	61	49	2.00×10^5
	60	50	2.00×10^5
	61	50	2.00×10^5
Death Valley	26	25, 26	6.07×10^4
	27	25	6.07×10^4
Upper and Middle Region	28	24, 25	6.07×10^4
	29	24	6.07×10^4
	30	23, 24	6.07×10^4

TABLE B.3. (Contd)

Geographic Location	Line	Column	Discharge (ft^3/day/Node)
Lower Region	14	28	6.14×10^4
	15	28	6.14×10^4
	16	28	6.14×10^4
	17	28	6.14×10^4
	18	28	6.14×10^4
	19	27	6.14×10^4
	20	27	6.14×10^4
	21	27	6.14×10^4
	22	26	6.14×10^4
Evapotranspirtation Discharges per Node			
Pahrump Valley	12	50	5.56×10^3
	14	48	1.11×10^4
	15	47	1.11×10^4
	16	48	1.33×10^4
	17	48	5.89×10^4
	16	46	2.22×10^4
	17	47	4.45×10^4
	18	46	1.11×10^4
	19	46	1.11×10^4
	20	46	1.11×10^4
	17	45	8.89×10^4
	19	42	3.89×10^4
	20	42	1.11×10^4
Furnace Creek Wash Area	27	26	8.64×10^4
	26	27	4.32×10^4
Ash Meadows	24	35	6.03×10^4
	25	36	6.03×10^4
Alkali Flat	19	37	1.98×10^5
	20	37	1.98×10^5
	20	38	1.98×10^5
	21	37	1.98×10^5
	21	38	1.98×10^5
	22	38	1.98×10^5
Indian Spring Valley	29	54	6.56×10^4
Three Lakes Valley (Corn Creek Springs)	25	61	4.64×10^4

TABLE B.3. (Contd)

Geographic Location	Line	Column	Discharge (ft^3/day/Node)
Mesquite Flat	33	19	1.0×10^3
	34	19	1.0×10^3
	35	19	1.0×10^3
Amargosa Desert	26	41	7.67×10^4
	27	41	7.67×10^4
	28	41	7.67×10^4
Sarcobatus Flat	46	23	1.58×10^5
	47	22	1.58×10^5
	47	23	1.58×10^5
	48	22	1.58×10^5
Oasis Valley	39	29	7.96×10^4
	40	29	7.96×10^4
	41	29	7.96×10^4
	42	29	7.96×10^4
	42	30	7.96×10^4
	43	30	7.96×10^4
Sand Spring Valley	63	52	1.00×10^4
	64	52	1.00×10^4
Railroad Valley	69	46	1.00×10^4
	70	46	1.00×10^4

APPENDIX C

CYCLIC STEADY-STATE ACTUAL EVAPOTRANSPIRATION AND RECHARGE CALCULATION

The Thornthwaite and Mather (1955) linear relationship for determining actual evapotranspiration (AET) depends on the soil moisture status of the soil (i.e., the ratio of the moisture content over the soil root-zone water-holding capacity). Because the antecedent soil moisture conditions are unknown, it is impossible to predict current soil moisture conditions. Therefore, we allow the AET and recharge calculations to cycle yearly until the soil moisture conditions reach what we will term 'cyclic steady state.' To start the cycle, we assume the soil moisture on January 1 to be - 1 inch less than the soil root-zone water-holding capacity. The calculation of AET is then allowed to cycle through as many years as necessary until the soil moisture content on December 31 is within 0.01 inch of the soil moisture on January 1 of the cycle. The convergence of the cycle to steady state usually occurs within two or three cycles or iterations.

Table C.1 shows the results of the cyclic steady-state calculation for AET and recharge. The iterations presented in Table C.1 are for the recharge results of the regional model that were previously presented in Table A.8. Table C.1 shows the soil moisture status on January 1 and December 31 of each year to clarify the convergence of the soil moisture content at each iteration. Convergence to cyclic steady-state soil-moisture conditions occurs in two iterations for this particular node.

Table C.2 further clarifies the AET and recharge calculation by providing the water balance calculations that are performed for each month. The details of the water balance calculation presented in Table C.2 are for the month of January of the first iteration of the yearly cycle presented in Table C.1. Table C.2 also refers to the appropriate figures and tables of this report that provide the actual numbers used in the AET and recharge calculation for the month of January of iteration 1.

TABLE C.1. Example of the Convergence Process used in the Actual Evapotranspiration and Recharge Calculation for One Node of the Regional Model

Node Location: near the base of the Spring Mountains
Vegetation Type: pinyon-pine/juniper
Soil type: mountains/foothills
Soil root-zone water-holding capacity: 2.2 in.

ITERATION NUMBER 1

Soil Moisture Content
January 1 = 1.200 in.
December 31 = 0.719 in.
Difference = 0.481 in. (convergence does not occur)

Month	Rainfall (in.)	PET (in.)	AET (in.)	Soil Moisture (in.)	Recharge Plus Runoff (in.)
January	1.6327	0.5968	0.5968	2.2000	0.0359
February	1.8801	0.7597	0.7597	2.2000	1.1204
March	2.9686	0.9011	0.9011	2.2000	2.0674
April	1.3194	1.8285	1.8285	1.6908	0.0000
May	2.1390	2.2150	2.1974	1.6325	0.0000
June	0.0990	2.8132	1.7314	0.0000	0.0000
July	0.6762	3.2552	0.6762	0.0000	0.0000
August	1.3804	2.8190	1.3804	0.0000	0.0000
September	0.9730	2.1545	0.9730	0.0000	0.0000
October	1.2188	1.3664	1.2188	0.0000	0.0000
November	1.4398	0.9069	0.9069	0.5328	0.0000
December	0.7092	0.5232	0.5232	0.7188	0.0000

Annual Rainfall = 16.44 in.
Annual PET = 20.14 in.
Annual AET = 13.69 in.
Annual Runoff = 0.00 in.
Annual Recharge = 3.22 in.

Table C.1 (Contd)

ITERATION NUMBER 2

Soil Moisture Content
January 1 = 0.719 in.
December 31 = 0.719 in.
Difference = 0.000 in. (convergence occurs)

Month	Rainfall (in.)	PET (in.)	AET (in.)	Soil Moisture (in.)	Recharge Plus Runoff (in.)
January	1.6327	0.5968	0.5968	1.7547	0.0000
February	1.8801	0.7597	0.7597	2.2000	0.6751
March	2.9686	0.9011	0.9011	2.2000	2.0674
April	1.3194	1.8285	1.8285	1.6908	0.0000
May	2.1390	2.2150	2.1974	1.6325	0.0000
June	0.0990	2.8132	1.7314	0.0000	0.0000
July	0.6762	3.2552	0.6762	0.0000	0.0000
August	1.3804	2.8190	1.3804	0.0000	0.0000
September	0.9730	2.1545	0.9730	0.0000	0.0000
October	1.2188	1.3664	1.2188	0.0000	0.0000
November	1.4398	0.9069	0.9069	0.5328	0.0000
December	0.7092	0.5232	0.5232	0.7188	0.0000

Annual Rainfall = 16.44 in.
Annual PET = 20.14 in.
Annual AET = 13.69 in.
Annual Runoff = 0.00 in.
Annual Recharge = 2.74 in.

TABLE C.2. Example of Monthly Water Balance Calculation[a]

Parameter	Value	Reference
Annual Rainfall	16.436 in.	Figure A.2
Monthly Fraction of Rainfall (January)	0.099	Figure A.4
Annual Potential Evapotranspiration (PET)	52.0 in.	Figure A.3
Monthly Fraction of PET (January)	0.023	Figure A.7
Crop Coefficient (January) (for pinyon pine/juniper)	0.507	Table A.5
Annual Runoff	0.00 in.	Figure A.11
Soil Root-Zone Water-Holding Capacity (SRWHC)	2.20 in.	Table A.7
Soil Moisture Content (January 1)	1.20 in.	Table C.1

CALCULATIONS

January Rainfall = Annual Rainfall x Monthly Fraction
= 16.436 (in.) x 0.099
≅ 1.63 (in.)

January PET (for pinyon pine/juniper) = Annual PET x Monthly Fraction x Crop Coefficient
= 52.0 (in.) x 0.023 x 0.507
= 0.59 (in.) (within round off error)

Soil Moisture (January 31) = Soil moisture (January 1) + Rainfall (January)
= 1.20 (in.) + 1.63 (in.)
= 2.83 (in.)

Thornthwaite and Mather (1955) Relationship for Actual Evapotranspiration Calculation (AET):

$$AET = PET \times \frac{\text{soil moisture}}{SRWHC}$$

with this condition:

$$\frac{\text{soil moisture}}{SRWHC} \leq 1.0$$

AET (January 31) = 0.59 (in.) x $\left(\frac{2.83}{2.20}\right)$
= 0.59 (in.) x 1.0
≅ 0.59 (in.)

Recharge (January 31) soil moisture - SRWHC - AET - Runoff
= 2.83 (in.) - 2.20 (in.) - 0.59 (in.) - 0.00 (in.)
= 0.40 (in.) (within roundoff error)

(a) The values presented in this table are for the month of January for Iteration 1 of Table C.1.

DOE/TIC-4500, UC-70 (336)

DISTRIBUTION LIST

J. W. Bennett (RW-20)
Acting Associate Director
Geologic Repository Deployment
U. S. Department of Energy
Washington, D. C. 20545

Ralph Stein (RW-21)
Acting Deputy Associate Director
Geologic Repository Deployment
U. S. Department of Energy
Washington, D. C. 20545

M. J. Lawrence (RW-1)
Acting Director
Office of the Director
U. S. Department of Energy
Washington, DC 20545

C. R. Cooley (RW-24)
Acting Director
Geosciences & Technology Division
Geologic Repository Deployment
U. S. Department of Energy
Washington, D.C. 20545

M. W. Frei (RW-23)
Acting Director
Engineering & Licensing Division
Geologic Repository Deployment
U.S. Department of Energy
Washington, D.C. 20545

J. J. Fiore (RW-22)
Acting Director
Program Management Division
Geologic Repository Deployment
U.S. Department of Energy
Washington, D.C. 20545

E. S. Burton (RW-25)
Acting Director
Siting Division
Geologic Repository Deployment
U.S. Department of Energy
Forrestal Building
Washington, D.C. 20585

R. P. Longo (RW-22)
Program Management Division
Geologic Repository Deployment
U. S. Department of Energy
Washington, D. C. 20545

Cy Klingsberg (RW-24)
Geosciences and Technology Division
Geologic Repository Deployment
U. S. Department of Energy
Washington, D. C. 20545

J. E. Shaheen (RW-25)
Institutional Relations Staff
Geologic Repository Deployment
U. S. Department of Energy
Forrestal Building
Washington, D.C. 20585

Chief, High-Level Waste Technical
Development Branch
Division of Waste Management
U. S. Nuclear Regulatory Commission
Washington, D.C. 20555

NTS Project Manager
High-Level Waste Technical
Development Branch
U.S. Nuclear Regulatory Commission
Washington, D.C. 20555

Document Control Center
Division of Waste Management
U.S. Nuclear Regulatory Commission
Washington, D.C. 20555

J. O. Neff
Salt Repository Project Office
U.S. Department of Energy
505 King Avenue
Columbus, OH 43201

ONWI Library (5)
Battelle Columbus Laboratory
Office of Nuclear Waste Isolation
505 King Avenue
Columbus, OH 43201

O. L. Olson, Project Manager
Basalt Waste Isolation Project Office
U.S. Department of Energy
Richland Operations Office
P.O. Box 550
Richland, WA 99352

E. B. Ash
Rockwell International Atomics
Rockwell Hanford Operations
Richland, WA 99352

A. A. Metry, Program Manager
Roy F. Weston, Inc.
2301 Research Blvd., 3rd Floor
Rockville, MD 20850

D. C. Newton (RW-23)
Engineering and Licensing Division
Geologic Repository Deployment
U. S. Department of Energy
Washington, DC 20545

R. R. Loux, Jr., Manager
Nuclear Waste Project Office
State of Nevada
Capitol Complex
Carson City, NV 89710

SAI-T&MSS Library (2)
Science Applications, Inc.
2950 South Highland Drive
Las Vegas, NV 89109

N. E. Carter
Battelle Columbus Laboratory
Office of Nuclear Waste Isolation
505 King Avenue
Columbus, OH 43201

S. A. Mann, Manager
Crystalline Rock Project Office
U.S. Department of Energy
9800 S. Cass Avenue
Argonne, IL 60439

L. D. Ramspott (3)
Technical Project Officer for NNWSI
Lawrence Livermore National
Laboratory
P.O. Box 808
Mail Stop L-204
Livermore, CA 94550

D. C. Hoffman
Los Alamos National Laboratory
P.O. Box 1663
Mail Stop E-515
Los Alamos, NM 87545

D. T. Oakley (3)
Technical Project Officer for NNWSI
Los Alamos National Laboratory
P.O. Box 1663
Mail Stop F-671
Los Alamos, NM 87545

Barry Gale (RW-25)
Siting Division
Geologic Repository Deployment
U.S. Department of Energy
Forrestal Building
Washington, DC 20585

K. Street, Jr.
Lawrence Livermore National
Laboratory
P.O. Box 808
Mail Stop L-209
Livermore, CA 94550

A. R. Hakl
Technical Project Officer for NNWSI
Westinghouse Electric Corporation
Waste Technology Services Division
Nevada Operations
P.O. Box 708
Mail Stop 703
Mercury, NV 89203

W. W. Dudley, Jr. (3)
Technical Project Officer for NNWSI
U.S. Geological Survey
P.O. Box 25046
418 Federal Center
Denver, CO 80225

J. A. Cross, Manager
Las Vegas Branch
Fenix & Scission, Inc.
P.O. Box 15408
Las Vegas, NV 89114

M. E. Spaeth (2)
Technical Project Officer for NNWSI
Science Applications, Inc.
2769 South Highland Drive
Las Vegas, NV 89109

W. S. Twenhofel
820 Estes Street
Lakewood, CO 80215

D. L. Vieth, Director (6)
Waste Management Project Office
U.S. Department of Energy
P.O. Box 14100
Las Vegas, NV 89114

D. F. Miller, Director
Office of Public Affairs
U.S. Department of Energy
P.O. Box 14100
Las Vegas, NV 89114

D. A. Nowack (14)
Office of Public Affairs
U.S. Department of Energy
P.O. Box 14100
Las Vegas, NV 89114

B. W. Church, Director
Health Physics Division
U.S. Department of Energy
P.O. Box 14100
Las Vegas, NV 89114

A. E. Gurrola, General Manager
Energy Support Division
Holmes & Narver, Inc.
P.O. Box 14340
Las Vegas, NV 89114

H. D. Cunningham
General Manager
Reynolds Electrical &
Engineering Co., Inc.
P.O. Box 14400
Mail Stop 555
Las Vegas, NV 89114

William W.-L. Lee
Roy F. Weston, Inc.
2301 Research Boulevard
Third Floor
Rockville, Maryland 20850

R. J. Blaney (RW-22)
Program Management Division
Geologic Repository Deployment
U. S. Department of Energy
Washington, DC 20545

P. T. Prestholt
NRC Site Representative
1050 East Flamingo Road
Suite 319
Las Vegas, NV 89109

T. Hay, Executive Assistant
Office of the Governor
State of Nevada
Capitol Complex
Carson City, NV 89710

C. H. Johnson
Nuclear Waste Project Office
State of Nevada
Capitol Complex
Carson City, NV 89710

Abby Johnson
414 West Ninth Street
Carson City, NV 89701

John Fordham
Desert Research Institute
Water Resources Center
P.O. Box 60220
Reno, NV 89506

Dr. Martin Mifflin
Desert Research Institute
Water Resources Center
Suite 201
1500 East Tropicana Avenue
Las Vegas, NV 89109

J. L. Younker (25)
Science Applications, Inc.
2769 S. Highland Drive
Las Vegas, NV 89101

G. Tomsic
Utah Dept. of Community
Economic Development
Room 6290, State Office Bldg.
Salt Lake City, UT 89114

P. J. Iverson, Deputy Director
Department of Minerals
State of Nevada
400 West King Street
Carson City, NV 89710

C. H. George
Geologic Repository Division
U.S. Department of Energy
S-10
Washington, DC 20545

H. E. Ransom
Energy Programs Division
U.S. Department of Energy
Richland, WA 99352

J. G. Vlahakis
Geologic Repository Division
U.S. Department of Energy, S-10
Washington, D.C. 20545

Battelle Memorial Institute (25)
Pacific Northwest Laboratory
P.O. Box 999
Richland, WA 99352
Attn: F. H. Dove (3)
D. W. Dragnich
M. D. Freshley
P. C. Hays
M. R. Kreiter
W. A. Rice
J. A. Stottlemyre
L. L. Wendell
Technical Information
Library (5)
Publishing Coordination (2)

P. L. Aamodt (2)
Los Alamos National Laboratory
Post Office Box 14100
Las Vegas, NV 89114

1500 W. Herrmann
1510 D. B. Hayes
1511 J. W. Nunziato
1520 T. B. Lane
1522 R. L. Johnson
1524 W. N. Sullivan
1524 R. K. Thomas
6300 R. W. Lynch
6310 T. O. Hunter
6311 L. W. Scully
6311 L. Perrine (2)
6311 R. I. Brasier
6311 A. W. Dennis
6311 T. W. Eglinton
6311 J. L. Jackson
6311 H. R. MacDougall
6311 A. R. Morales
6311 J. T. Neal
6311 P. D. O'Brien
6311 C. G. Shirley
6311 V. J. Stephens
6311 K. D. Young
6312 F. W. Bingham
6312 N. K. Hayden
6312 B. S. Langkopf
6312 Y. T. Lin
6312 R. R. Peters
6312 S. Sinnock
6312 M. S. Tierney (3)
6312 J. G. Yeager
6313 J. R. Tillerson
6313 J. A. Fernandez
6313 F. B. Nimick
6313 R. M. Zimmerman
6314 G. K. Beall
6314 A. J. Mansure
6330 WNWSICF
3141 C. M. Ostrander (5)
3151 W. L. Garner (3)
8424 M. A. Pound